

Ultra-fast Boriding for Improved Energy Efficiency and Reduced Emissions in Materials Processing Industries. Final Report.

Project Period: 9/30/2008 – 9/30/2011 (extended to 12/31/2011)

Energy Systems Division

About Argonne National Laboratory

Argonne is a U.S. Department of Energy laboratory managed by UChicago Argonne, LLC under contract DE-AC02-06CH11357. The Laboratory's main facility is outside Chicago, at 9700 South Cass Avenue, Argonne, Illinois 60439. For information about Argonne and its pioneering science and technology programs, see www.anl.gov.

Availability of This Report

This report is available, at no cost, at <http://www.osti.gov/bridge>. It is also available on paper to the U.S. Department of Energy and its contractors, for a processing fee, from:

U.S. Department of Energy
Office of Scientific and Technical Information
P.O. Box 62
Oak Ridge, TN 37831-0062
phone (865) 576-8401
fax (865) 576-5728
reports@adonis.osti.gov

Disclaimer

This report was prepared as an account of work sponsored by an agency of the United States Government. Neither the United States Government nor any agency thereof, nor UChicago Argonne, LLC, nor any of their employees or officers, makes any warranty, express or implied, or assumes any legal liability or responsibility for the accuracy, completeness, or usefulness of any information, apparatus, product, or process disclosed, or represents that its use would not infringe privately owned rights. Reference herein to any specific commercial product, process, or service by trade name, trademark, manufacturer, or otherwise, does not necessarily constitute or imply its endorsement, recommendation, or favoring by the United States Government or any agency thereof. The views and opinions of document authors expressed herein do not necessarily state or reflect those of the United States Government or any agency thereof, Argonne National Laboratory, or UChicago Argonne, LLC.

Ultra-fast Boriding for Improved Energy Efficiency and Reduced Emissions in Materials Processing Industries. Final Report.

Project Period: 9/30/2008 – 9/30/2011 (extended to 12/31/2011)

prepared by
Ali Erdemir, Osman Eryilmaz, and Vivekanand Sista
Energy Systems Division, Argonne National Laboratory
and
Bodycote Thermal Processing, Inc.

August 2012

Work sponsored by
Advanced Manufacturing Office (formerly Industrial Technologies Program)
Office of Energy Efficiency and Renewable Energy, U. S. Department of Energy
under Award No. DE-PS36-08GO98014

Final Technical Report

Ultra-Fast Boriding for Improved Energy Efficiency and Reduced Emissions in Materials Processing Industries

Authors:

Ali Erdemir, Argonne National Laboratory, Energy Systems Division, Argonne, IL 60439; Phone (630) 252-6571, Fax: (630) 252-5568, erdemir@anl.gov

Osman Eryilmaz, Argonne National Laboratory, Energy Systems Division, Argonne, IL 60439; Phone (630) 252- 91 27, Fax: (630) 252-5568, eryilmaz@anl.gov

Vivekanand Sista, Argonne National Laboratory, Energy Systems Division, Argonne, IL 60439; Phone (630)252-1741, Fax: (630) 252-5568, vsista@anl.gov

Industrial Collaborator:

Bodycote Thermal Processing, Inc., 12700 Park Central Drive (Suite 700), Dallas, Texas, 75251-1518, USA

DOE Award Number: CPS Agreement No. 17882

Project Period: 9/30/2008 – 9/30/2011 (extended to 12/31/2011)

Date of Report: August 2012

Acknowledgment: This report is based upon work supported by the U.S. Department of Energy under Award No.DE-PS36-08GO98014. Many dedicated scientists, engineers, technicians, and students have contributed to the project. In particular, Gregory Krumdick, Gerald Jeka, Jeff Spangenberger, and Scott Lockwood have played significant roles in various stages of the project and contributed toward its success. Bodycote personnel including Mario Ciampini, Ken Beard, Ed Jamieson, Nicholas Bugliarello and Craig Zimmerman were also very helpful in process scale-up, field demonstration, and technology transfer and commercialization stages of the project. We also acknowledge Dr. Edward J. Daniels and William D. Ingle of Argonne for their help and guidance during the course of this project.

Disclaimer: Any findings, opinions, and conclusions or recommendations expressed in this report are those of the author(s) and do not necessarily reflect the views of the Department of Energy.

Table of Contents

Executive Summary	8
Introduction	10
Background.....	12
Results and Discussion.....	15
<i>Technical Approach</i>	15
<i>Process Development and Optimization</i>	15
<i>Structural Studies</i>	16
<i>Optimization of Boriding Rate</i>	20
<i>Mechanical, Tribological, Adhesion, and Corrosion Studies</i>	22
<i>Boriding of Odd-shaped and Pre-carburized Steel</i>	26
<i>Assessment of Residual Stress</i>	26
<i>Design and Construction of Industrial-scale Boriding Unit</i>	28
(i) <i>Selection of Sand Layer (Reaction Zone)</i>	34
(ii) <i>Design and Manufacture of Anode, Cathode, Busbars, and Other Fixtures</i>	36
(iii) <i>Production-scale Furnace</i>	39
<i>Boriding of Parts for Field Evaluation</i>	42
Benefits Assessment.....	46
Commercialization	48
Accomplishments	49
Conclusions	51
Recommendations	52
References	53

Lists of Figures

- Figure 1.** Progression of boriding units from a 1.5-in. to 20-in. size.....16
- Figure 2.** Microstructural evolution of boride layer as a function of treatment time.17
- Figure 3.** General photo of a knife guard and sections cut from two of the teeth. Note that the surfaces are clean, and any residue left has been washed away in water...17
- Figure 4.** (a) General and (b) higher-magnification (50X) images of boride layer formed on a pre-carburized industrial part.....18
- Figure 5.** Ultra-fast borided piston ring segments and the cross-sectional morphology of the thick boride layer formed on the surface. It took only 30 min to achieve such a thickness.....18
- Figure 6.** Microstructure of boride layer (a) after a 15-min boriding experiment showing both FeB (darker phase near the top) and Fe₂B (lighter phase beneath) and (b) after leaving the same sample in the bath for 45 min (no FeB layer is left). Bath composition of 10% Na₂CO₃ + 90% Na₂B₄O₇; current density of 200 mA/cm²; bath temperature of 950°C.....19
- Figure 7.** (a) General photo of the pilot-scale boriding unit and (b) industrial parts being loaded and (c) recovered from the unit after boriding treatment.19
- Figure 8.** Cross-sectional images of (a) boride layer formed after 15 min of boriding and (b) the same layer after 45 min soaking in the electrolyte. Darker contrasting phase near the top in (a) is due to FeB phase, while the white contrasting layer in (b) is due to Fe₂B, which is the most desired phase for industrial applications. Note that during that additional soaking, the layer became much thicker, suggesting that boron diffusion into the substrate steel continued.....20
- Figure 9.** Relationship between boride layer thickness and time at different boriding temperatures. Bath composition of 10% Na₂CO₃ + 90% Na₂B₄O₇; current density of 200 mA/cm²; substrate material of AISI 1018 steel.....21
- Figure 10.** Relationship between boride layer thickness and current density. Bath composition of 10% Na₂CO₃ + 90% Na₂B₄O₇; duration of 5 min; temperature of 950°C; substrate material of AISI 1018 steel.....21
- Figure 11.** Physical condition of (a) as-received and (b) borided AISI 1018 steel substrate after dipping into a 15% HCl containing water solution for 3 h at room temperature. The as-received sample was severely corroded while the borided sample was still shiny and protected against corrosion.22
- Figure 12.** (a) 3D image and (b) line scan of wear track formed on untreated AISI 1018 steel subjected to a wear test under 5 N load and at 6.3 cm/s sliding velocity against an alumina ball. The sliding distance was 225 m. Note that the z-axis in line scan over the worn area is in micrometers; same holds for Figs. 13-15.....22
- Figure 13.** (a) 3D image and (b) line scan of wear track formed on carburized AISI 1018 steel subjected to a wear test under 5 N load and at 6.3 cm/s sliding velocity against an alumina ball. The sliding distance was 225 m.23
- Figure 14.** (a) 3D image and (b) line scan of wear track formed on conventionally borided (pack borided) AISI 1018 steel substrate subjected to a wear test under 5 N load and at 6.3 cm/s sliding velocity against an alumina ball. The sliding distance was

	225 m.....	23
Figure 15.	(a) 3D image and (b) line scan of wear track formed on borided AISI 1018 steel substrate subjected to a wear test under 5 N load and at 6.3 cm/s sliding velocity against an alumina ball. The sliding distance was 225 m.	23
Figure 16.	Microscopic images of wear track formed on (a) nitro-carburized, (b) carburized, (c) conventional (pack) borided, and (d) ultra-fast borided samples under lubricated sliding conditions (fully formulated 5W30 oil, 52100 steel ball, 50 N load, 1.5 cm/s velocity, and 225 m sliding distance).....	24
Figure 17.	Abrasion resistance of borided D2 and unborided D2 samples.	24
Figure 18.	Condition of borided steel after Rockwell C indentation: (a) 15 min boriding only and (b) 15 min boriding plus 45 min soaking.	25
Figure 19.	Cross-section hardness profile of a sample that was borided for 15 min and then left in the electrolyte for additional 45 min. As is clear, the transition from hard phase on the top to soft substrate is very gradual and smooth.....	26
Figure 20.	Cross-section micrographs of sharp corners of a knife guard after ultra-fast boriding (verifying the formation of dense, uniform, and thick boride layers).	27
Figure 21.	(a) Cross-sectional image of a carburized and then ultra-fast borided knife guard that was subjected to hardening heat treatment after boriding and (b) microhardness profile of the same sample as a function of depth from surface.	27
Figure 22.	Cross-sectional images of boride layers consisting of (a) single Fe ₂ B phase and (b) dual FeB+Fe ₂ B phases used in the stress measurement experiments.....	28
Figure 23.	Schematic of (a) fixture for 32 knife guards in one holder, (b) complete design for 96 knife guards, and (c) knife guards loaded in the production-scale unit.	29
Figure 24.	Schematic of square production unit (open top on left and fully assembled with top furnace cap assembly on right).	30
Figure 25.	Schematic of furnace cap assembly showing details of electrodes and other fixtures.	31
Figure 26.	Schematic of (a) individual part holder (cathode) and (b) graphite anode and cathode assemblies together.	31
Figure 27.	Electrolyte contamination problem, evidenced by greenish color upon solidification.	33
Figure 28.	Surface condition of a high-quality, dense SiC brick after 72-h continuous testing in molten electrolyte. No evidence of brick failure or corrosion in and around the splash zone.....	33
Figure 29.	Surface condition of (a) KX-99 (aluminum silicate-based brick) and (b) Narmag 60 (MgO and Cr ₂ O ₃ -based brick) after 3-h testing in molten electrolyte. Both of these bricks failed and corroded away rapidly. In the case of Narmag 60, we also had the same discoloration problem (most likely due to Cr ₂ O ₃).	34
Figure 30.	Schematic of furnace wall layers and their functions.	35
Figure 31.	(a) Schematic of electrical connections from power supply to furnace top cover (top view) and (b) side view of the same.	37
Figure 32.	(a) Schematic of power distribution to cathodes and anodes and (b) saddles to	

	be used for delivering power to cathode and anode racks.....	37
Figure 33.	General photos of both nickel rods that were tested as anode and cathode materials.....	39
Figure 34.	Completed production-scale boriding furnace. The SiC heaters (three on each side) as well as busbars for electrical connection are on top.....	40
Figure 35.	Schematic of part holder and a photo of actual cutters to be used in large-scale boriding trials.	40
Figure 36.	Photo of the preheating furnace (top) and the power supply (bottom left) and the computer-controlled power rack (bottom right) as they are being assembled.	41
Figure 37.	Photo of the fully assembled production-scale boriding furnace.....	41
Figure 38.	Industrial parts being taken out of the industrial-scale boriding unit after a boriding process.....	42
Figure 39.	Borided cutters recovered from pilot-scale boriding furnace (top). Four short (left) and four long (right) middle finger cutters that were borided in 90% borax + 10% sodium carbonate electrolyte at 950°C.....	42
Figure 40.	Sectioned cutter and its cross-sectional micrographs from the tip of region 2 (top, right) and from regions 1, 2, and 3 (bottom, from left to right).....	43
Figure 41.	Hardness profile of sectioned John Deere cutter from top surface to interior. Within the borided layer, the hardness is around 1400 Vickers, while that of the carburized layer beneath is 800 Vickers.....	44
Figure 42.	Experimental setup for electrochemical boriding of ball valve (left) and borided ball valve (right) showing clean surface finish after washing in hot water.	44
Figure 43.	Other industrial parts that were successfully treated by ultra-fast boriding: (a) engine piston pin, (b) titanium textile guide, and (d) engine tappet.....	45

List of Tables

Table 1. Residual compressive stress levels in boride layers.....28

Table 2. Performance characteristics of various materials tested for anode and cathode holders.....,38

Table 3. Key properties of large-scale boriding compared with other surface treatment processes.....46

Executive Summary

High-temperature treatment processes (such as nitriding, carburizing, and boronizing) are well-established and used widely by numerous industrial sectors to achieve superior mechanical and tribological properties on all kinds of engineering components made out of ferrous materials. Unfortunately, these traditional processes are very slow and energy intensive, and they produce large amounts of CO₂ emissions and liquid/solid wastes to deal with during and after each process run. From economic and environmental points of views, it is highly desirable to develop and implement novel surface treatment technologies that are quick, cheap, clean, and energy efficient. The main objective of this project was to develop an industrial-scale ultra-fast boriding process that realizes all of these desirable attributes. The other objectives of the project were to demonstrate the superior performance, properties, and durability of borided surfaces under relevant test conditions and to transfer optimized technology to industry for large-scale practice. Major research activities included process design, modeling, product optimization, and scale-up.

This project has achieved all of its stated objectives, and the industrial-scale boriding process has been successfully transferred to industry. Specifically, all of the original tasks have been completed, and the milestones have been met by scaling up from a small proof-of-concept system (which could only handle about 0.25 kg melt) to a commercial-scale boriding unit that can handle up to 4,000 kg melt. Mechanical and tribological testing of borided test samples and industrial parts has also been carried out, and their superior performance over a broad range of test conditions has been validated. With the large-scale, ultra-fast boriding process, we could achieve thick, hard, and uniform boride layers on all kinds of steel components, even after only 5 min of treatment time. We could also attain excellent uniformity in thickness over the entire exposed surfaces — even in the very sharp corners or interior sections of odd-shaped workpieces. Boriding of numerous nonferrous materials was also demonstrated, and thick boride layers (up to 300 μm in thickness) were achieved on their outer surfaces.

With the use of a large-scale boriding unit at Argonne National Laboratory, our research team has successfully treated large numbers of industrial components in a batch-to-batch operation without creating any in-house gaseous emissions or producing solid and/or liquid wastes. With the use of this large unit, our team achieved surface hardness values of 15 to 45 GPa, depending on the type of metal or alloy being treated. The thick boride layers attained on steel components consisted of FeB, Fe₂B, and Fe₃B phases, and their hardness values ranged from 16 to 22 GPa. Layers consisting of Fe₂B phase alone are also possible with this process, and in the case of nonferrous materials. Overall, because of the much superior property and performance improvements in treated products, much lower energy consumption, and nearly zero environmental waste and emissions, the demonstrated boriding technology may find broad applications in many cross-cutting industries. Mechanical wear, abrasion, erosion, corrosion, and scuffing are often life-limiting factors in mechanical systems that are used in manufacturing, transportation, aerospace, agricultural, earth-moving, and mining equipment; but the machine components treated by ultra-fast boriding can effectively prevent such degradations.

In this project, the ultra-fast boriding was proven to be most ideal for the treatment of iron and many other ferrous alloys, like stainless steel. We have shown through our experimental studies that our method can also be used for the treatment of many nonferrous metals and alloys. In the case of superalloys and Ni₃Al intermetallic materials, more than a 300-μm thick boride layer can be achieved with our boriding furnace within 15 to 30 min (which results in five times the hardness of the base materials). Pre-carburized steels and nonferrous alloys can also be treated by the new boriding technique. Overall, very thick (more than a quarter millimeter) and hard surface layers produced by ultra-fast boriding are expected to have a positive impact on

the performance and durability of all types of machine components that are subject to corrosive, erosive, abrasive, and adhesive wear. Since the focus of our project was primarily on the large-scale boriding of ferrous materials, in this report, we will broadly cover the results from various ferrous materials that were used in our experiments.

Another transformational feature of ultra-fast boriding is that it does not create any greenhouse gas emissions or solid and/or liquid wastes to deal with during or after the treatment; hence, it is an ultra-green technology (no need for expensive waste disposal and/or treatment facilities). It may eliminate the use of natural gas and other carbon-based fuels as the primary energy source in the heat treatment industry (which is the most common practice at present), thus, minimizing the CO₂, NO_x, CO, and SO_x emissions that are generated in large quantities by current heat treatment practices. The main ingredient used during boriding is borax, which is a natural mineral.

Our demonstrated and scaled-up technology can now be used in a wide range of manufacturing and transportation applications. It can deliver thick and uniform boride layers of more than 200 μm in steels, if needed, over the entire exposed surfaces — even in the very sharp corners or interior sections of workpieces (which are typical of gears, tools, pipes, and other components). Beneath the distinct boride layers is an equally-thick boron diffusion layer or zone, which is comparable to the diffusion zones achieved by carburizing and nitriding processes. In the cases of traditional boriding, nitriding, and/or carburizing methods, achieving such layer thickness and case depths would have taken several hours, and these surfaces would not have achieved the same levels of hardness and other desirable properties as they do with ultra-fast boriding.

Some of the key stakeholders of ultra-fast boriding technology include companies that are active in heat-treatment, thermal-diffusion, and hard-coating processes; metal-forming, machining, and other manufacturing processes; and technologies related to transportation (including original equipment manufacturers for autos), mining and oil exploration, agricultural and heavy equipment. Bodycote Thermal Processing was the cost-sharing industrial partner and licensee in this project. They also provided test components and technical and commercial information pertaining to industrial components that are most suitable for ultra-fast boriding. Bodycote also coordinated some of the field tests and metallurgical examinations.

Overall, ultra-fast boriding is a transformational technology that can complement, if not replace, many of the energy- and carbon-intensive surface treatment processes that are in use today, such as conventional boriding, carburizing, nitriding, carbo-nitriding, and physical and chemical vapor deposition. In our project, the developed technology was scaled-up and proven to be an ultra-green, ultra-efficient process that can drastically reduce costs, increase productivity, and improve the performance and reliability of machine components used in cross-cutting industrial applications.

Introduction

In response to the Department of Energy (DOE) Lab Call (DE-PS36-08GO98014) on Energy Intensive Processes in 2008, Argonne National Laboratory prepared and submitted a research proposal to DOE focused on scale-up and commercialization of an ultra-fast boriding process. Compared to traditional thermal-treatment processes, this process offered the potential to reduce boriding duration from hours to minutes and drastically reduce energy consumption and CO₂ emissions. Due to its ability to deliver very dense, thick, and hard boride layers, this process could also provide much improved performance and durability in many types of machine tools and other industrial components. If scaled up successfully, companies involved in heat and/or surface treatments could greatly benefit from this technology and achieve higher productivity, lower cost, and much superior competitive edge in the global marketplace. Much improved mechanical properties enabled by ultra-fast boriding could also substantially increase product life, which indirectly reduces cost and energy consumption due to the elimination of the frequent repair and/or re-manufacturing of failed parts.

Conventional boriding processes such as pack, paste, plasma, fluidized bed, and salt-bath boriding are cumbersome, environmentally unsafe, and energy intensive; in addition, they are slow and limited in their ability to create a dense and thick boride layer [1]. For example, conventional pack boriding (which is the most popular boriding process) requires several steps for a successful boriding run and takes more than 6 hours to produce a 45- μm -thick boride layer on a low-carbon steel part. Despite the operational difficulties, high cost, and energy and carbon intensities, pack boriding has so far been the most dominant boriding process for the treatment of industrial parts. Other boriding processes mentioned above are not used for large-scale industrial purposes. The most common boron-yielding or -releasing powders used in pack boriding include boron carbide (B₄C), ferroboration, and amorphous boron [2]. The powder mixture also uses a variety of diluents such as silicon carbide (SiC) and aluminum oxide (Al₂O₃) powders, as well as numerous catalyzers or boron activators such as sodium fluoroborate (NaBF₄), potassium fluoroborate (KBF₄), ammonium fluoroborate [(NH₄)₃BF₄], ammonium chloride (NH₄Cl), sodium carbonate (Na₂CO₃), and barium fluoride (BaF₂). (Many of these compounds are considered environmentally hazardous, requiring extensive and costly safety measures for industrial hygiene in workplaces and for workers.) Furthermore, conventional boriding requires a great deal of time and effort to precisely pack the parts into a boriding powder mix and then, after the boriding process, to clean them from the boriding powders, which have to be discarded safely. Cleaned parts are heated above 900°C and then quenched for hardening and tempering heat treatments to achieve high hardness in base steel. In ultra-fast boriding, these additional steps can be done right after the boriding process without any interruptions, as an integral part of the boriding process.

The conventional boriding process is labor-intensive. Handling or packing powders around the work pieces in the beginning poses serious environmental health and safety concerns for the workplace. Also, the stuck-on or fused powders are very difficult to remove from the surface of treated parts (especially the highly articulated and intricate parts) after boriding. Rigorous grit-blasting and/or abrasive grinding is required to remove them from the surface. Even with these steps, the surface finish tends to be rough and undesirable for high precision applications. Pack boriding may also cause warping and extensive micro-crack formation on finished products due to long exposure to high temperatures. Compared to conventional boriding and other energy- and carbon-intensive surface treatments, ultra-fast boriding is a green and efficient technology. It does not produce any gaseous emissions (including greenhouse or other hazardous gases), nor are there any solid and/or liquid wastes. As will be elaborated later, the key ingredient used in ultra-fast boriding is a natural borax mineral, which is cheap, safe, and abundant.

In addition to being very thick, the boride layers produced by ultra-fast boriding are dense and uniform in microstructure, and they have excellent mechanical hardness (depending on the type of steel, up to 22 GPa is feasible), as well as wear and corrosion resistance — even under very harsh operating conditions. For comparison, the mechanical hardness of a typical nitrided and/or carburized surface is in the range of 6.5 to 11 GPa. Undoubtedly, ultra-fast boriding offers many advantages, including increased productivity, reduced cost, and lowered gaseous emissions, relative to today's long heat-soak technologies such as pack boriding, carburizing, and nitriding.

The main objective of our project was to scale up and commercialize an ultra-fast boriding process that could overcome most of the difficulties and deficiencies associated with pack boriding. This process also offered the potential to provide as much as 80% higher energy efficiency than pack boriding, near-zero emissions in workplaces, and much higher productivity and product quality. Furthermore, we aimed to demonstrate cost-competitiveness of the ultra-fast borided surfaces, as well as superior property, performance, and durability characteristics. In our exploratory studies, we were able to validate the ultra-fast nature of our boriding process in tests using an R&D-size boriding unit that could handle 250 g molten electrolyte. For our process to be industrially viable, however, it had to be scaled up. To reach that goal, we partnered with an industrial heat treatment company and collaborated to rapidly scale up and deploy our technology for large-scale utilization. Together, we demonstrated its scalability, cost competitiveness, and superior property, performance, and durability characteristics, and then we licensed and transferred optimized technology.

The ultra-fast boriding process was proven to be the best for the treatment of iron- and steel-based materials, but it can also be used for the treatment of certain nonferrous metals and their alloys (e.g., titanium, tantalum, zirconium, tungsten, niobium, molybdenum, magnesium, most nickel-based and cobalt-based superalloys, and cobalt-chrome alloys) and cermets. Pre-carburized, nitrided, and carbo-nitrided steels can also be treated by the new boriding technique. Thick (up to quarter-millimeter thick) and hard surface layers produced by ultra-fast boriding can have a significant positive impact on the performance and durability of many mechanical components that are subject to harsh operating conditions involving erosion, corrosion, and abrasion. These conditions are typical of operations in mining and oil drilling, forest products, construction, agriculture, and earth moving. Such coatings can also be used in a wide range of transportation applications for which high resistance to wear and scuffing is paramount.

Overall, the large-scale boriding process has been proven to be ultra-fast, clean, efficient, and low-cost. Hence, it constitutes an ideal alternative to existing high-temperature materials processing and advanced manufacturing practices that currently rely on more energy-intensive heat treatment and coating methods, which also generate huge amounts of greenhouse gases and solid and liquid wastes. Realizing all of these positive attributes, our industrial collaborator, Bodycote Thermal Processing, has finalized licensing negotiations with Argonne and adopted this technology for full-scale industrial practice.

Background

Among the many surface and/or thermal treatment processes available today, nitriding, carburizing, and boriding (or boronizing) represent some of the most popular processing technologies for high-temperature materials, and they are used extensively by many industrial sectors to achieve superior surface mechanical and tribological properties in all kinds of machine parts and components [1-3]. Other surface engineering processes such as thermal and/or plasma spraying, plasma-transferred arc, laser glazing, electron-beam deposition, physical vapor deposition (PVD), chemical vapor deposition (CVD), etc., are also used widely to enhance the near-surface properties of machine components [4]. Unfortunately, these surface treatment processes are slow (it may take several hours to achieve desired thicknesses or case depths) and expensive. They are also energy intensive, and in the case of carburizing, nitriding, and boriding, they are not considered environmentally friendly since they generate large amounts of liquid and/or solid wastes and release large volumes of gaseous emissions to the environment.

Most of the surface treatment processes mentioned above require several heating-cooling steps during operation and, hence, require long processing time to achieve reasonably thick case depths with desirable surface properties. For example, in a typical carburizing process, parts to be treated are often heated to fairly high temperatures (ranging from 500 to 1100°C) and held there for a very long time (which may vary from a few hours to 60 hours or more). After the carburizing cycle, there are additional steps involving cooling of the treated parts to room temperature and then heating them up again in a different furnace for quenching and tempering. Depending on the applications, stress-relieve annealing and sub-zero treatment are employed to eliminate retained austenite. In general, these conventional processes are cumbersome, time consuming, energy-intensive, environmentally harmful, and as a result, very expensive.

Like nitriding and carburizing, the boriding is an important surface treatment process in which boron atoms diffuse into the near surface regions of a workpiece and react with the metallic constituents there to form a thick layer essentially composed of hard boride phases. In the case of ferrous alloys, boride layer consists primarily of Fe_2B and FeB phases [1]. A thick boron diffusion zone also exists beneath the top boride layers and provides good mechanical support for the top layers. Iron borides are chemically stable and mechanically perhaps the hardest form of all iron compounds. Therefore, when present as a dense layer on a surface, these boride layers can substantially increase the resistance of these surfaces to corrosive, adhesive, abrasive, and erosive wear. Process conditions (such as duration of boriding, process temperature, and surface and bulk compositions of materials being treated and the composition of boriding media) may all affect the chemistry and thickness of the resultant boride layers.

At present, several kinds of boriding methods are available (such as salt-bath boriding, fluidized-bed boriding, pack boriding, paste boriding, and gas-phase and plasma discharge boriding) for the production of hard boride layers on appropriate substrates [2]. These methods are based primarily on the use of a variety of boron-rich solid, liquid, or gaseous compounds. Fluidized bed-, pack-, and paste-boriding methods use solid boron compounds (such as B_4C , amorphous boron, and ferro-boron) and other chemicals during the boriding process, while plasma boriding uses gaseous boron compounds in a plasma discharge environment.

Among all other boriding techniques, pack boriding is the one that is most widely used by industry. It is a mature technology and typically done in sealed or packed retorts at very high temperatures. A typical pack has large amounts (about 90%) of boron carrier powder materials (like SiC), a source of boron (like boron carbide or amorphous boron), and an activator (like

KBF₄) to enhance diffusion of atomic boron into the workpiece [1,2,5]. Pack boriding involves placing the workpieces into the powder mix and sealing them in a container. The container is then heated up to around 950°C and held there for 4 to 8 hours and finally cooled in air. The thickness of the boride layers is determined by the process temperature and duration but typically is in the range of 50 to 100 μm. Powders used in the pack pose difficult waste management and disposal problems and are not easy to recycle or reuse. In the case of salt-bath boriding, a molten salt bath consisting of 60 to 70 wt% borax, 10 to 15 wt% boric acid, and 10-20 wt% ferro-silicon or ferro-boron is used at temperatures ranging from 900 to 1000°C. Boride layers forming on the surface are typically 10-15 μm thick after 7 to 10 hours of treatment [6].

Borided steels consistently outperformed their nitrided and carburized counterparts in comparative wear studies, mainly because of their much higher hardness (16 to 20 GPa) as compared to carburized or nitride steels whose hardness values are in the range of 7 to 11 GPa. In fact, the hardness of borided layers is comparable to that of transition metal nitride and carbide coatings produced by various PVD and CVD methods. The TiB₂ that forms on the surface of borided titanium substrates may achieve hardness values higher than 30 GPa. The high hardness values afforded by these boride layers are retained up to 650°C. Since there is no discrete or sharp interface between the boride layer and base material, adhesion strengths of boride layers to base metals are always strong, and interfacial failure is not an issue. Compared to nitrided and carburized surfaces, borided surfaces provide much higher resistance to oxidation and corrosion.

Materials that are most suitable for boriding include all types of ferrous metals and alloys like low- and high-carbon steels; low- and high-alloy steels; tool steel; stainless steels; carburized, nitrided, and carbo-nitrided steels; and cast irons. Nonferrous metals and their alloys like titanium, tantalum, zirconium, tungsten, niobium, molybdenum, most nickel-based and cobalt-based superalloys, cobalt-chrome alloys, tungsten and sintered carbides, and/or cermets may also be borided with the use of an appropriate boriding process. However, the thickness of the boride layer may be shallow, and the structure is porous or full of defects.

Despite their abilities to produce much harder and more wear- and corrosion-resistant surface layers, traditional boriding methods such as pack boriding are not used as widely by industry as compared to nitriding and carburizing processes. Many inherent problems have hindered the more widespread use of the boriding process. Chief among them is the very high cost of boriding (5 to 6 times more expensive than carburizing and nitriding). Beside the high cost, very long processing times (up to 20 hours), toxic emissions/byproducts, and poor surface condition of finished products (including surface cracks, flaking, etc.) have also been important factors in the limited use of this method. For these reasons, it would be desirable to develop a new and much improved boriding method that is fast, cheap, clean, and applicable to a wide range of materials.

To address all of the difficulties and shortcomings mentioned above, we focused our attention on the scale-up of an ultra-fast boriding process. We had to also demonstrate cost-competitiveness, as well as superior property, performance, and durability characteristics, of the ultra-fast borided surfaces, and in the end we were able to transfer optimized technology to an industrial partner for large-scale applications in several industrial fields.

As the name implies, the ultra-fast boriding process is very fast; in a low carbon steel (AISI 1018) sample, it can produce 90- to 100-μm-thick boride layers within 30-40 minutes. The traditional pack-boriding method would have taken more than 10 hours to achieve similar boride

layer thicknesses. Ultra-fast boriding uses a simple electrochemical cell operating at high current density (50 to 700 mA/cm²) and low voltage (1-15 V). The main ingredients of the molten electrolyte for the cell are mainly borax, Na₂B₄O₇ (70-90 wt.%), and sodium carbonate, Na₂CO₃ (10-30 wt%). These chemicals are very cheap and non-toxic (naturally occurring), and do not result in any type of hazardous emissions or wastes. In addition, small amounts (0.1 to 5 wt%) of alkaline and/or alkaline-earth halides (CaCl₂, NaCl, KCl, etc.) may also be used in place of or in addition to sodium carbonate to accelerate the boriding process. Specifically, the addition of these halides into molten electrolyte results in a significant increase in the boriding rates and refines the grain size and morphology of the borided surface layers. These halides release large amounts of Cl ions into the electrolyte and, hence, increase electrical conductivity and surface transport activities on metal surfaces and thereby increase boron intake or diffusion. The Cl ions also ensure uniform current distribution across the electrolyte (this is very important for achieving uniform case depths on very intricate or odd-shaped workpieces). The halide additives also make it easy to clean the workpieces after the boriding process. Since the borided parts are all water soluble, rinsing them in running water is sufficient to remove any residue that may have been present on the surface.

Ultra-fast boriding can be used to treat all kinds of metallic and alloy surfaces, including ferrous alloys, titanium base alloys, nickel-based and cobalt-based superalloys, tantalum, zirconium, molybdenum, tungsten, niobium, hafnium, and rhenium (boriding of Mg and Al alloys is under consideration, but will require a lower temperature process/electrolyte). These borided metals and alloys can have a huge positive impact on all kinds of manufacturing and transportation applications, such as metal forming tools, fuel injectors, gears, bearings, and power- and drive-train components in cars and trucks. Boride layer thicknesses as high as 0.25 mm are feasible. Such a thick and hard borided surface layer can prevent wear and scuffing between heavily loaded rolling, rotating, or sliding surfaces under lubricated sliding conditions which are typical of these engine components. One of the most important features of these borided surfaces is their ability to function under severe loading conditions and provide low friction and wear with and without lubrication. As stated earlier, ultra-fast boriding process is environmentally benign. There are no toxic raw materials to be used during boriding and no by-products to be discarded afterwards. The process also does not produce any hazardous emissions or greenhouse gases. In other boriding processes, new baths are needed (in the case of salt-bath boriding), and the old ones must be discarded properly. In the case of pack boriding, huge amounts of greenhouse gases are produced, and the powders and active boron sources must be disposed of properly. In the case of gas-phase boriding, there are some toxic gases that need to be handled very carefully. One of the other advantages of the ultra-fast boriding is that the electrolyte can be re-used multiple times, although borax as a rich boron source needs to be replenished occasionally. Again, the new process is environmentally friendly, and there are no toxic by-products to discard or deal with after the process. Minor electrolyte materials or deposits left on the surfaces of the treated metals can be easily dissolved or washed away in water.

Results and Discussion

Technical Approach

In our much earlier exploratory studies using a very small proof-of-concept furnace, we had performed extensive boriding studies to confirm that ultra-fast chemical conversion rates can be achieved on a variety of steel samples. We had also carried out systematic mechanical and tribological studies on the borided samples and confirmed that their hardness, friction, and wear behaviors were much superior to those of carburized and nitrided steel samples. In the present DOE project, we primarily focused on the scalability and commercial viability of this process for large-scale industrial applications.

During Year 1, the main focus was on process scale-up and optimization. The specific goal was to design and develop two larger or medium-size boriding furnaces and to demonstrate the feasibility of processing several test samples or batches of smaller industrial parts at once. In particular, acquiring a fundamental knowledge of how different process parameters can potentially affect the thickness, hardness, surface finish, structural/chemical nature, and tribological properties of the borided test samples was of great importance for gaining better confidence on the scalability and commercial viability of the process. Such an understanding could potentially provide a sound scientific basis for identifying and applying the most ideal combination of process parameters, which would, in turn, lead to the development of a robust and efficient process and the highest quality end-products. In short, during Year 1, we mainly attempted to gain a comprehensive understanding of the relationship between various process parameters and the mechanical and tribological characteristics of the borided steel surfaces.

The main objective of Year 2 activities was to concentrate more on technology scale-up, maturation, validation, and field performance testing of larger batches of industrial parts with the help of an industrial collaborator. In particular, we focused our attention on the design and construction of a pilot-scale production unit that could handle much bigger industrial parts and larger batches of smaller mechanical parts. We also conducted a series of long-duration performance and durability tests under conditions that were typical of some of the intended industrial applications. While doing all these, we obtained and tested numerous test samples treated by the traditional or competing technologies (including nitriding, carburizing, and pack boriding) and determined the extent of mechanical/tribological improvements in a comparative manner.

Toward the end of Year 2 and more particularly in Year 3, our main objective was to design and construct an industrial-scale boriding unit and demonstrate its viability for mass production. Specifically, we sought to demonstrate that ultra-fast boriding is feasible at industrial scales. Obviously, market acceptance and successful commercialization of a new technology depend on many other factors, but if we could demonstrate cost-competitiveness, energy efficiency, and environmental benefits of the new process, then the market acceptance/penetration should be relatively easy. Therefore, we had to confirm that the scaled-up process can easily treat many industrial parts in a cost-effective, efficient, and environmentally safe manner.

Process Development and Optimization

During Year 1, we concentrated our effort mostly on process scale-up and optimization. Specifically, we designed and constructed two medium-size boriding units (with much larger melt capacity) and successfully used them for the treatment of numerous test samples and

small batches of industrial parts at once. These units worked quite well and allowed us to perform numerous systematic studies directed toward understanding the effects of various process parameters on the boriding rate and on the boride layer quality and properties. Using the knowledge gained from these systematic studies, toward the end of Year 1, we initiated design of a pilot-scale boriding unit with much larger melt capacity. Figure 1 shows the progression of our research activities in designing and building of ever larger boriding units, from a very small 1.5-in. to a 20-in. diameter reactor, during Year 1 and 2.

During Year 1, we also conducted comprehensive mechanical and tribological studies on borided test samples to assess their mechanical properties and friction and wear performance under a wide range of test conditions. We also performed extensive structural and chemical characterization of the borided surfaces using a variety of surface analytical tools. Effects of contact pressure, temperature, and other test parameters were examined in detail, and appropriate friction and wear charts were generated to show their property and performance characteristics. Details of these studies are presented in the following section.

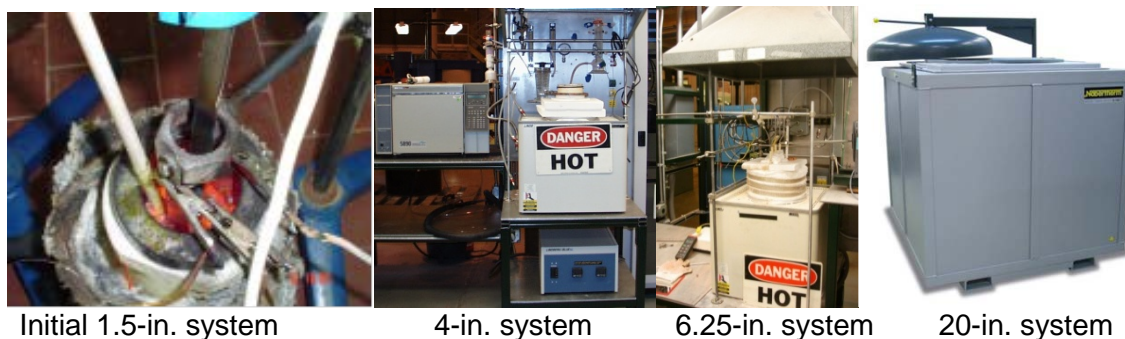


Figure 1. Progression of boriding units from a 1.5-in. to 20-in. size.

Structural Studies

Using the 4-in. boriding unit shown in Fig. 1, we tried boriding of test samples at different time intervals to establish the impact of process duration on boriding layer thickness at a given current density and boriding temperature. As shown in Fig. 2, we were able to achieve thick (15 μm) boride layers even after 5 min of treatment. After 30 min, the boride layer was more than 90 μm thick. The test sample treated for one hour exhibited a boride layer that was nearly 130 μm thick. Based on these positive developments early on, we attempted to treat some of the industrial parts furnished by Bodycote by using the intermediate-size (6.25-in.) boriding unit. Figures 3-5 show two of the industrial parts that were subjected to ultra-fast boriding and then cut into smaller pieces for metallographic examination.

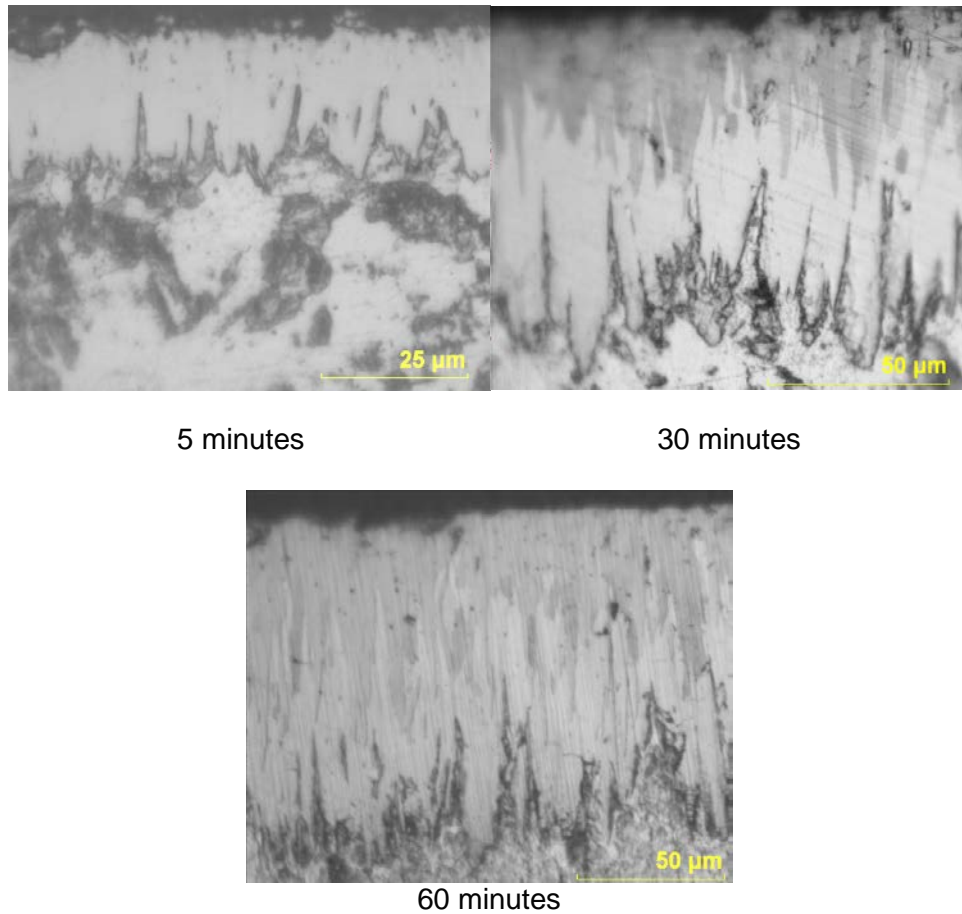


Figure 2. Microstructural evolution of boride layer as a function of treatment time.

As obvious from Figs. 3 to 5, we were able to produce thick (70-160 μm) boride layers on these industrial parts as well without any problems. It would have taken several hours to attain similar boride thickness by the conventional pack-boronizing process. These preliminary results were certainly encouraging and further sparked the interest of our industrial partner toward accelerating the project and ultimately building and installing a production-scale boriding unit in one of their heat-treatment plants.



Figure 3. General photo of a knife guard and sections cut from two of the teeth. Note that the surfaces are clean, and any residue left has been washed away in water.

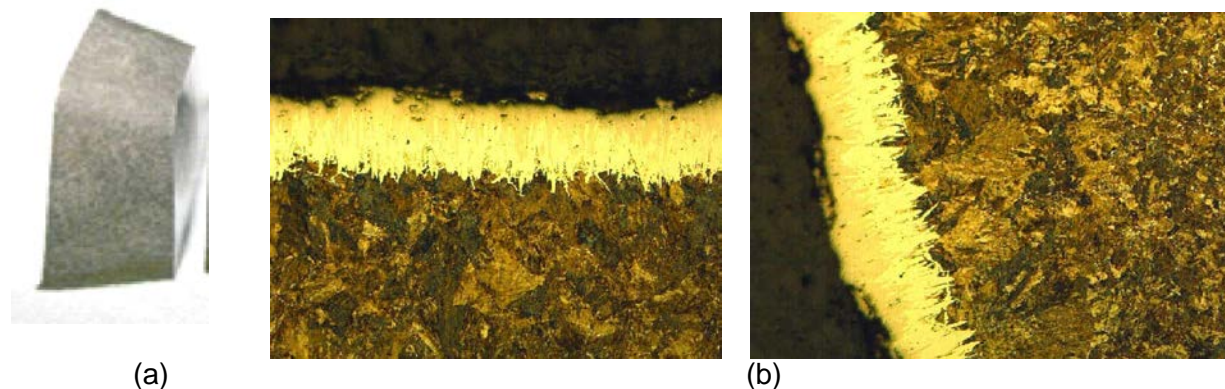


Figure 4. (a) General and (b) higher-magnification (50X) images of boride layer formed on a pre-carburized industrial part.

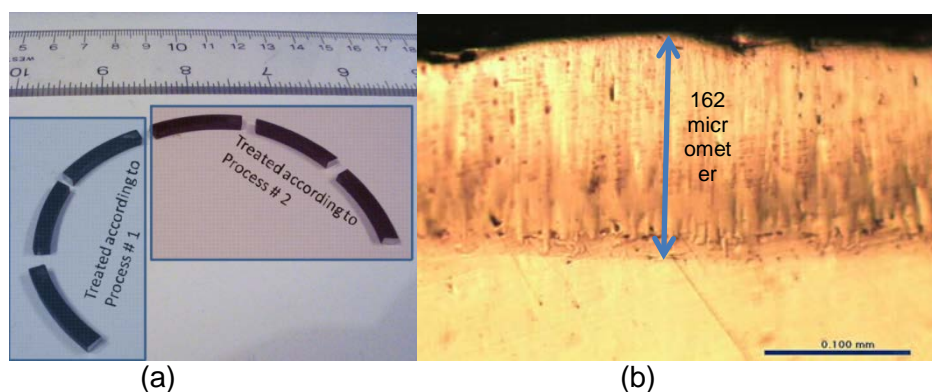


Figure 5. Ultra-fast borided piston ring segments and the cross-sectional morphology of the thick boride layer formed on the surface. It took only 30 min to achieve such a thickness.

Boride layers formed during our experiments on steel samples consisted of two boride phases: FeB and Fe₂B (see Fig. 6). According to Bodycote, for most wear protective applications, the Fe₂B phase is more desirable than the FeB (mainly because of the former's greater toughness). To achieve the single-phase Fe₂B in borided steels, we followed a procedure of first doing a short-duration boriding (say 15 min) and then switching off the power source and leaving the borided samples in the electrolyte for 30 to 45 min. In the end, we realized that the whole borided layer was totally converted to the Fe₂B phase, as shown in Fig. 6b.

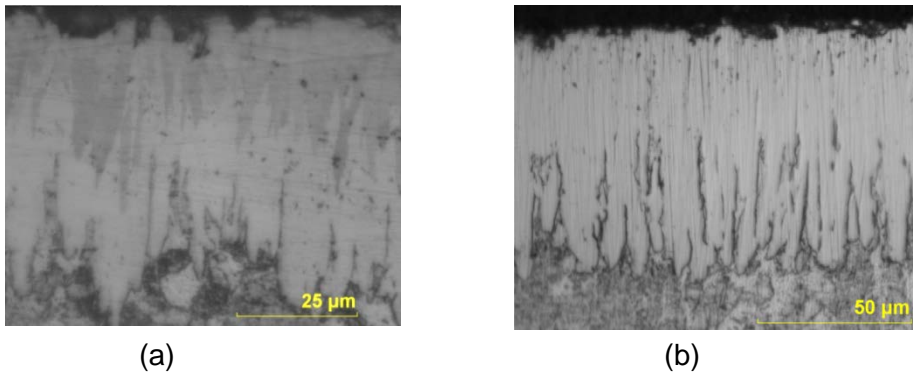


Figure 6. Microstructure of boride layer (a) after a 15-min boriding experiment showing both FeB (darker phase near the top) and Fe₂B (lighter phase beneath) and (b) after leaving the same sample in the bath for 45 min (no FeB layer is left). Bath composition of 10% Na₂CO₃ + 90% Na₂B₄O₇; current density of 200 mA/cm²; bath temperature of 950°C.

Based on these impressive results, toward the end of Year 1, we began to design a pilot-scale boriding furnace to demonstrate the feasibility of processing larger batches of test samples and/or industrial parts at once. This was one of the most immediate desires of our industrial partner. In our original plan, this task would have occurred toward the end of the second year, but again based on the very favorable results from the two smaller boriding furnaces, we decided to speed up our development work and begin the construction of a larger or pilot-scale boriding unit. Figure 7a shows a photograph of this boriding unit with its fully computerized control unit. After completing the instrumentation and installation of this larger furnace, we ran numerous boriding experiments to confirm that the process was still robust and able to produce very thick layers on all of the test samples and industrial parts that were tried. After finishing these initial studies, we initiated to boride large numbers of industrial parts to demonstrate its effectiveness in delivering equally thick and hard layers on the surfaces of these industrial parts. Figure 7b shows this new boriding furnace being prepared for an industrial boriding experiment, while Fig. 7c shows borided industrial parts being taken out of the furnace.

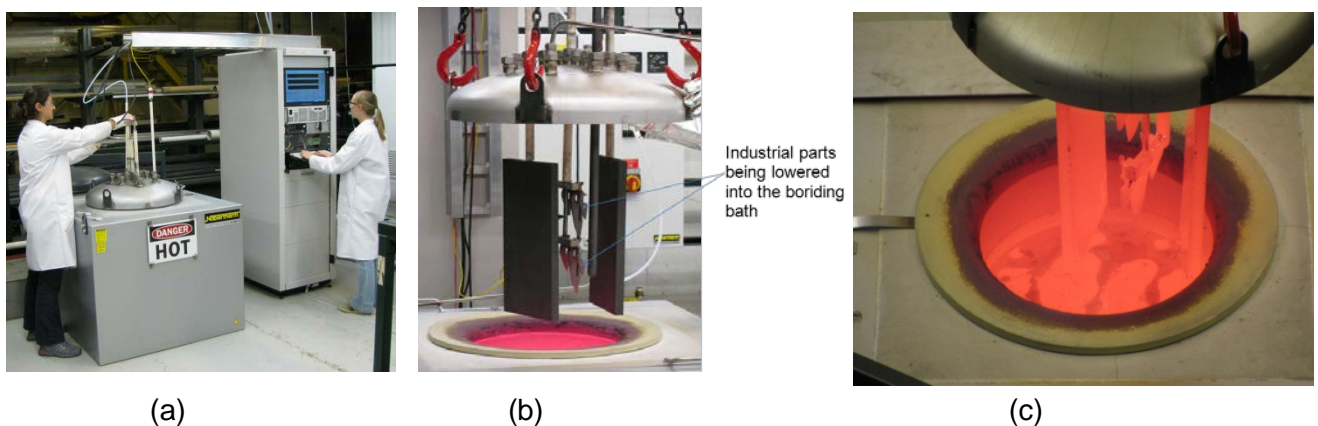


Figure 7. (a) General photo of the pilot-scale boriding unit and (b) industrial parts being loaded and (c) recovered from the unit after boriding treatment.

Structurally, the samples borided in this new pilot-scale unit exhibited somewhat thicker and more uniform boride layers than the ones that were treated in the smaller units for comparable boriding durations. The thickness of the boride layer was about 65 μm after 15 min of boriding, as shown in Fig. 8a. Note that this cross-sectional image also shows a darker FeB phase near the top. This phase is unavoidable in most boriding processes, but from a mechanical or tribological application point of view, it is also highly undesirable due to its poor fracture toughness. To eliminate it, we left the borided samples in the molten electrolyte for an additional 45 min, during which the whole boride layer was converted to Fe_2B , and the total layer thickness increased by an additional 25%. This sequential treatment led to the total elimination of the top FeB layer. As shown in Fig. 8b, this layer was not present during that additional 45 min soaking time. Glancing angle x-ray diffraction studies also confirmed that after the additional soaking, all of the FeB phase had been converted to Fe_2B phase, which is much tougher and hence most desired.

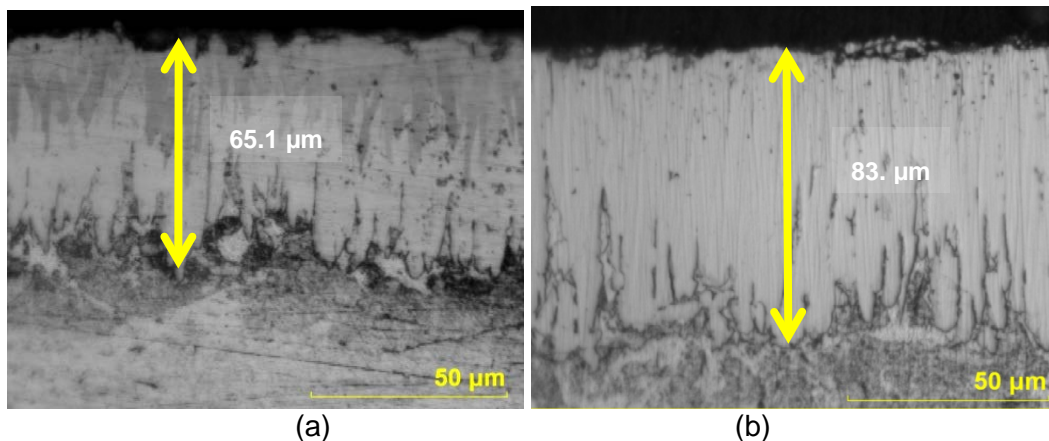


Figure 8. Cross-sectional images of (a) boride layer formed after 15 min of boriding and (b) the same layer after 45 min soaking in the electrolyte. Darker contrasting phase near the top in (a) is due to FeB phase, while the white contrasting layer in (b) is due to Fe_2B , which is the most desired phase for industrial applications. Note that during that additional soaking, the layer became much thicker, suggesting that boron diffusion into the substrate steel continued.

Optimization of Boriding Rate

Most the process optimization studies were carried out during Year 1. Specifically, we performed numerous boriding experiments over a wide range of process conditions to ascertain the effects of process parameters on boride layer thickness, composition, and microstructure as well as mechanical and tribological properties. For example, our studies on time vs. boride layer thickness showed that regardless of the bath temperature, the boride layer thickness grows nearly linearly with time during the first 30 min, but then drops slightly to follow another linear growth rate up to 120 min. Overall, as shown in Fig. 9, we achieved a boride layer thickness of about 250 μm in 120 min at 1000 $^{\circ}\text{C}$, while at 850 $^{\circ}\text{C}$, the growth rate and thickness were significantly lower.

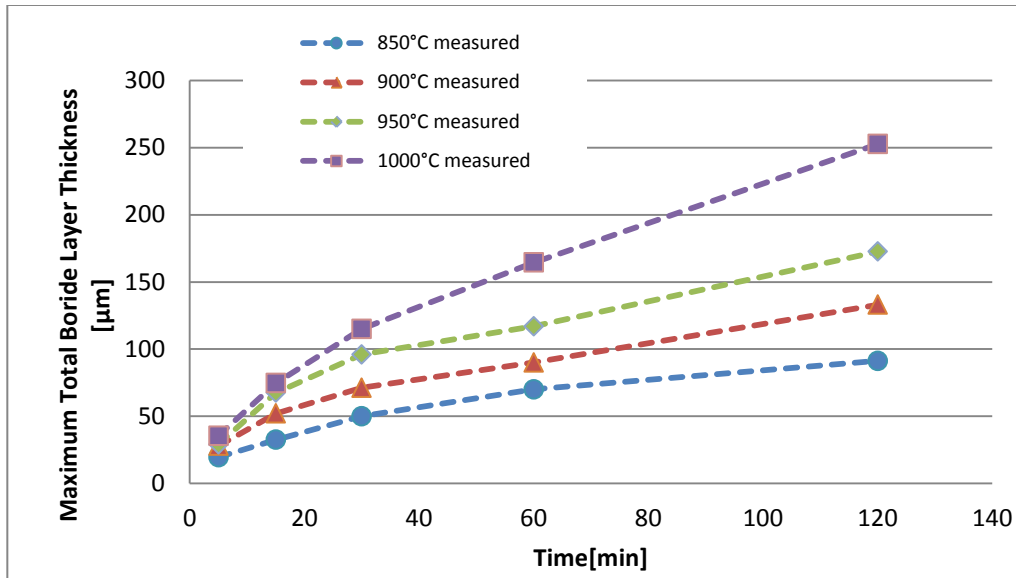


Figure 9. Relationship between boride layer thickness and time at different boriding temperatures. Bath composition of 10% Na_2CO_3 + 90% $\text{Na}_2\text{B}_4\text{O}_7$; current density of 200 mA/cm^2 ; substrate material of AISI 1018 steel.

Figure 10 shows the relationship between boride layer thickness and current density for a given time (5 min) and temperature (950°C). Up to 150 mA/cm^2 , the relationship is linear, but at much higher current densities, the linear relationship is still maintained but at a different slope. Overall, even for very short durations, e.g., 5 min, ultra-fast boriding process is capable of producing more than 20- μm -thick boride layers if desired at high current densities. Such a capacity is important for the treatment of certain industrial parts that require short and fast treatments and, hence, low overall cost. Based on these studies, for large-scale productions, perhaps a current density of 150 mA/cm^2 might be most appropriate since it delivers the fastest growth rate. In addition to the low-carbon steel samples, we tried many other steel types (including AISI 52100, D2, and H13) and achieved equally favorable results. We also borided nonferrous materials like superalloys, intermetallics, titanium and its alloys, cemented carbides, and cermets.

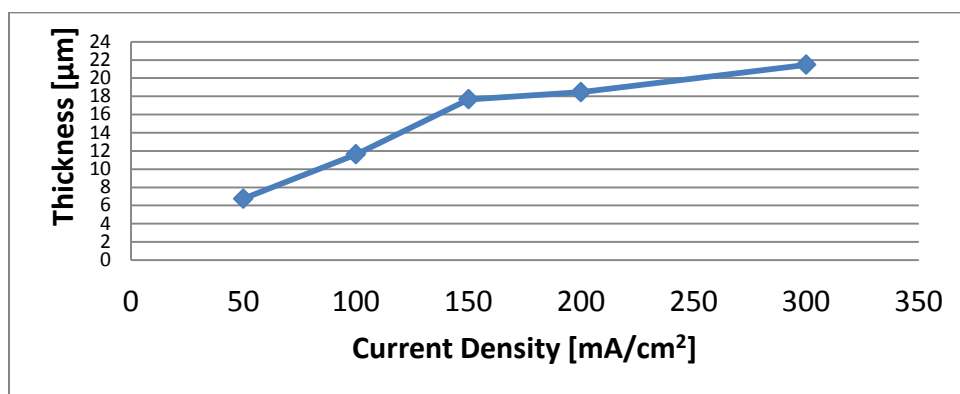


Figure 10. Relationship between boride layer thickness and current density. Bath composition of 10% Na_2CO_3 + 90% $\text{Na}_2\text{B}_4\text{O}_7$; duration of 5 min; temperature of 950°C; substrate material of AISI 1018 steel.

Mechanical, Tribological, Adhesion, and Corrosion Studies

We performed corrosion and tribological characterization of control and borided test samples that were specifically prepared for such studies. In our corrosion tests, borided 1018 steel samples demonstrated high resistant to corrosive attack. As shown in Fig. 11, even in 15% HCl containing water solutions, the borided test sample maintained its metallic appearance, while the control (unborided) steel sample had undergone severe corrosion, as it was totally rusted and covered with a dark corrosion product or rust.

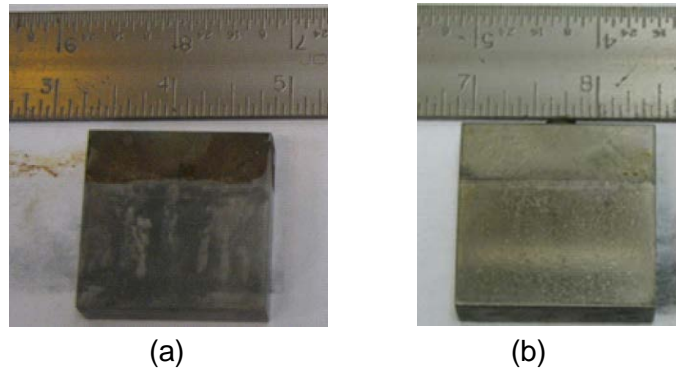


Figure 11. Physical condition of (a) as-received and (b) borided AISI 1018 steel substrate after dipping into a 15% HCl containing water solution for 3 h at room temperature. The as-received sample was severely corroded while the borided sample was still shiny and protected against corrosion.

Tribological characterization of borided test samples was performed with tribo-test machines in our laboratory. In one of these, we ran tests under dry sliding conditions to determine the wear resistance of control, carburized, conventional (pack) borided, and ultra-fast borided samples. As shown in Fig. 12, the unborided or control test sample wore out severely and formed a deep wear groove. The wear performance of the carburized test sample was also poor, as it formed a deep wear track as shown in Fig. 13. Figure 14 shows the wear performance of a steel sample treated by conventional pack boriding. This sample performed much better than the unborided control and carburized samples, exhibiting a much shallower wear groove. The best performance was attained by the ultra-fast borided sample, as shown in Fig. 15. Its wear groove was the shallowest, and its wear width was also the smallest of all.

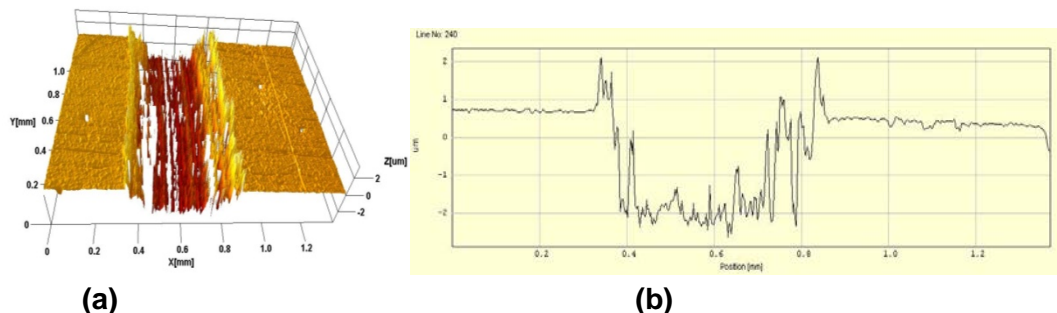


Figure 12. (a) 3D image and (b) line scan of wear track formed on untreated AISI 1018 steel subjected to a wear test under 5 N load and at 6.3 cm/s sliding velocity against an alumina ball. The sliding distance was 225 m. Note that the z-axis in line scan over the worn area is in micrometers; same holds for Figs. 13-15.

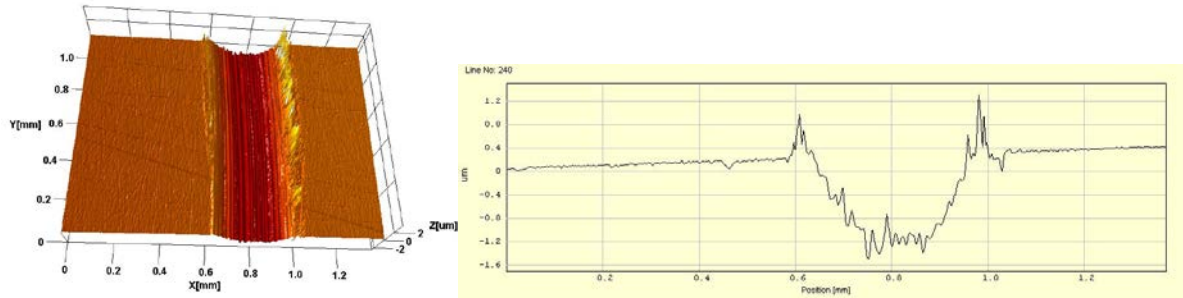


Figure 13. (a) 3D image and (b) line scan of wear track formed on carburized AISI 1018 steel subjected to a wear test under 5 N load and at 6.3 cm/s sliding velocity against an alumina ball. The sliding distance was 225 m.

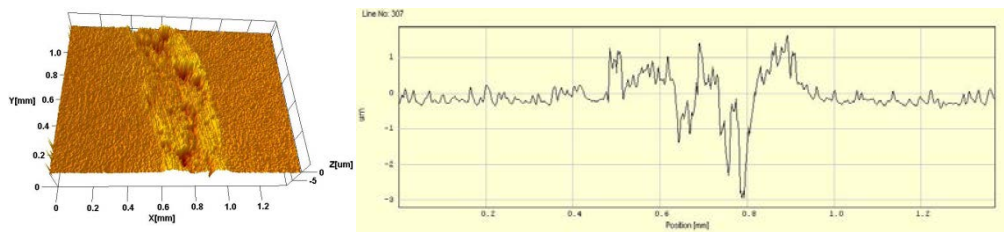


Figure 14. (a) 3D image and (b) line scan of wear track formed on conventionally borided (pack borided) AISI 1018 steel substrate subjected to a wear test under 5 N load and at 6.3 cm/s sliding velocity against an alumina ball. The sliding distance was 225 m.

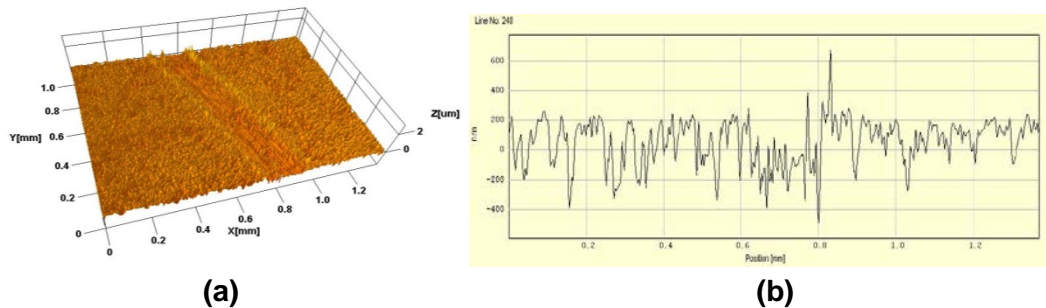


Figure 15. (a) 3D image and (b) line scan of wear track formed on borided AISI 1018 steel substrate subjected to a wear test under 5 N load and at 6.3 cm/s sliding velocity against an alumina ball. The sliding distance was 225 m.

Under lubricated sliding conditions, the ultra-fast borided surface provided the best protection against wear as compared to the other processes. As shown in Fig. 16, the sliding wear tracks of nitro-carburized, carburized, and conventional borided samples were very wide and showed evidence of mild wear, while the ultra-fast borided sample showed minor discoloration on the sliding wear track area but not much wear damage, thus confirming its wear resistance under lubricated sliding conditions.

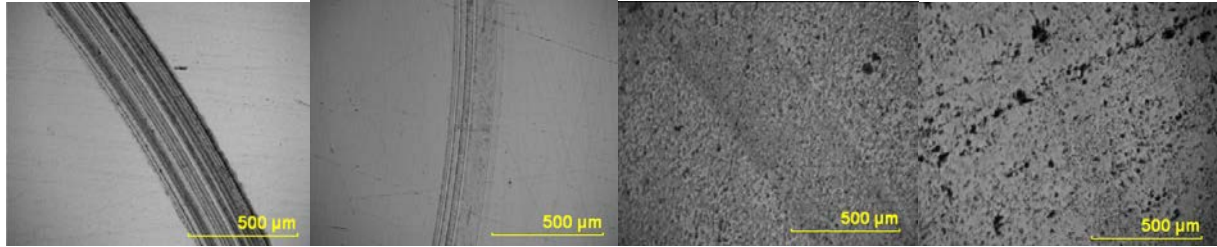


Figure 16. Microscopic images of wear track formed on (a) nitro-carburized, (b) carburized, (c) conventional (pack) borided, and (d) ultra-fast borided samples under lubricated sliding conditions (fully formulated 5W30 oil, 52100 steel ball, 50 N load, 1.5 cm/s velocity, and 225 m sliding distance).

To assess the abrasive wear resistance of borided steel samples, we performed three-body abrasion experiments on borided and control AISI D2 test samples. The boriding was done at 1000°C and current density of 200 mA/cm² for one hour. Control D2 samples had a hardness value on the Rockwell C scale of 61. These experiments were performed using ASTM G65A (“Standard Test Method for Measuring Abrasion Using the Dry Sand/Rubber Wheel Apparatus”) as a guideline. The total number of revolutions was varied from 2000 up to 6000, corresponding to sliding distances of 568 m to 1705 m. Mass loss was used to determine the amount of material removed due to abrasive wear. A graph displaying the volume loss in relation to sliding distance is given in Fig. 17. The volume loss with respect to sliding distance is much lower for the borided D2 samples than control samples, confirming the abrasion resistance of the borided test samples.

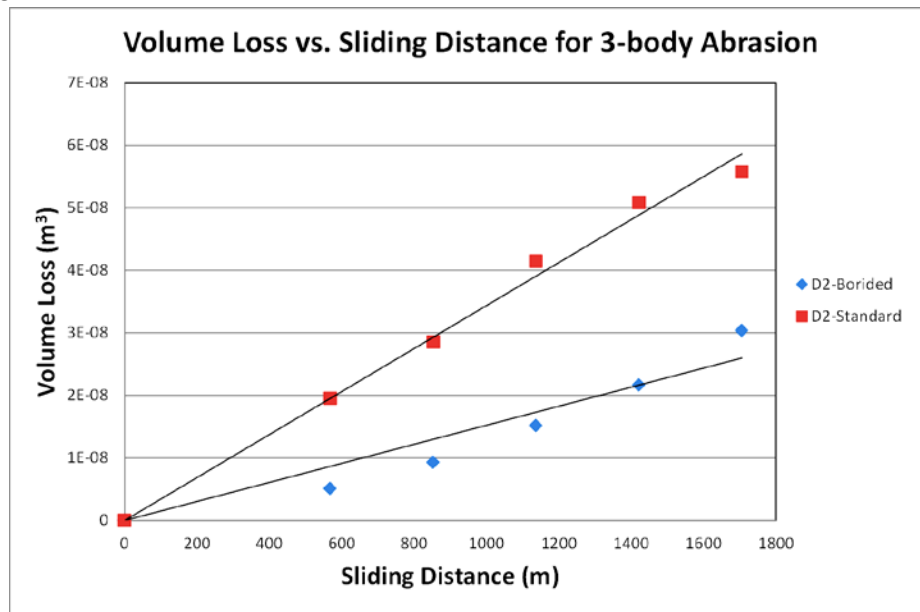


Figure 17. Abrasion resistance of borided D2 and unborided D2 samples.

The mechanical and adhesion characteristics of ultra-fast borided steel samples were determined by using a Rockwell C indentation machine. Specifically, the Daimler–Benz Rockwell-C (HRC-DB) adhesion test method was adopted to assess the adhesion properties of the boride layers formed on steel substrates. In this tester, a Rockwell “C”-type diamond

indenter was used under a load of 150 kg to create an indent. Subsequently, the indented spot was examined thoroughly using an optical microscope for signs of shattering or gross delamination failure.

Figure 18 shows the response of ultra-fast borided surfaces to Rockwell C indentation tests. As is clear from Fig. 18a, boride layers consisting of both FeB and Fe₂B phases do show some signs of crack formation, as well as severe fracture and chipping in and around the rim of the indented spot; there is no evidence of such behavior for the boride layer consisting of a single Fe₂B layer, which was achieved by soaking the borided test piece in the melt for 45 min, as shown in Fig. 18b. This test demonstrated the toughness of the Fe₂B phase in contrast to the brittleness of FeB.

Mechanically, the borided layers were found to be dense and hard. As shown in Fig. 19, the hardness of borided layer is around 16 GPa near the top surface for this predominantly Fe₂B-containing boride layer. For a layer composed of FeB on top and Fe₂B in the bottom, the top layer hardness would have been more than 20 GPa. However, as explained before, the FeB layer is brittle and, hence, is not desirable for mechanical applications. The transition from the hard top region to softer substrate was very gradual, which is desirable for industrial applications. If the transition is abrupt, premature fracture and delamination may occur and adversely impact the durability and performance of the borided surfaces.

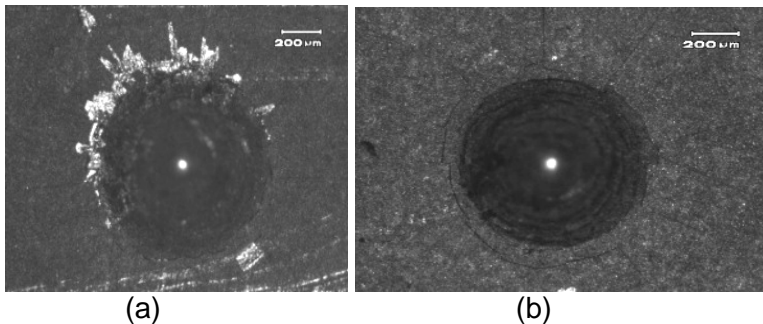


Figure 18. Condition of borided steel after Rockwell C indentation: (a) 15 min boriding only and (b) 15 min boriding plus 45 min soaking.

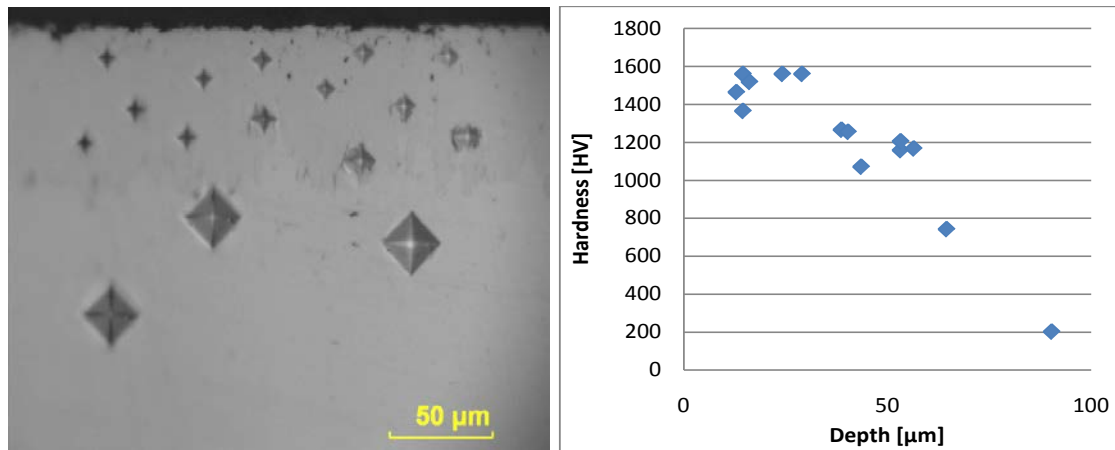


Figure 19. Cross-section hardness profile of a sample that was borided for 15 min and then left in the electrolyte for additional 45 min. As is clear, the transition from hard phase on the top to soft substrate is very gradual and smooth.

Boriding of Odd-shaped and Pre-carburized Steel

From an industrial point of view, the uniformity of boride layers over sharp corners and other intricate shapes is important. Furthermore, if boriding can be done on pre-carburized or nitrided steels, then the carburized or nitrided subsurface beneath can provide excellent mechanical support. Accordingly, we tried numerous test samples and industrial parts with odd shapes to see if boriding thickness is uniform over sharp edges and corners. In an industrial part with sharp edge, we were able to achieve a very thick (about 90 μm) and uniform boride layer on top of a pre-carburized part, as shown in Fig. 20. In fact, this particular part was subjected to a standard hardening heat treatment after boriding to achieve much higher hardness within the carburized subsurface. The sample was subsequently sectioned, then hardness measurements were taken with a Wilson micro-hardness test machine starting from the top surface to the interior. Figure 21a shows a cross-section image of the sectioned sample with all the indentation marks present. Figure 21b shows the hardness profile as a function of depth. As can be noticed, the top boride layer has the highest hardness value, around 1400 Vickers, while the hardness of carburized layer beneath is around 800 Vickers but decreases gradually with distance from the top surface. This experiment confirmed clearly that our boriding method is compatible with carburized steels and additional heat treatment processes. Also, we did not detect any cracks or evidence for any type of flaking or delamination of the top boride layer after such heat treatments (which involved heating to high temperatures and then rapidly quenching in water).

Assessment of Residual Stress

Another major objective was to elucidate the effect of process variables on structural chemistry and on the extent of residual stresses within the borided top surface layers. Specifically, the process conditions of our large boriding unit were adjusted in such a way that we could achieve thick boride layers consisting of only Fe₂B phase and a mixture of both Fe₂B and FeB phases, as shown in Fig. 22. On the basis of spectra from thin-film X-ray diffraction, we determined the residual stress levels in the boride layers. Table 1 compares the extent of residual stresses in

the layer with pure Fe_2B phase and the layer with Fe_2B and FeB phases. As is clear, the single-phase Fe_2B has more residual stress than the dual-phase $FeB+Fe_2B$. In the near future, we will perform mechanical and tribological tests on these borided steel samples to determine the effects of internal stress on friction, wear, and abrasion.

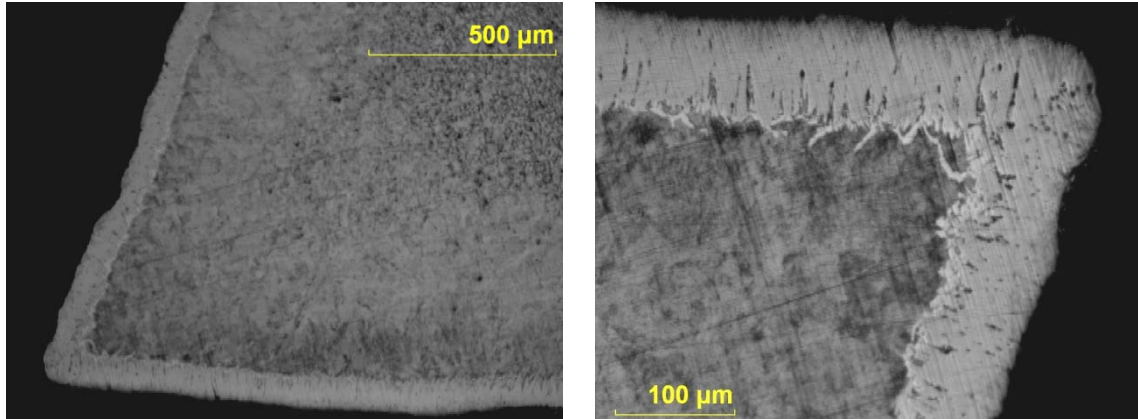


Figure 20. Cross-section micrographs of sharp corners of a knife guard after ultra-fast boriding (verifying the formation of dense, uniform, and thick boride layers).

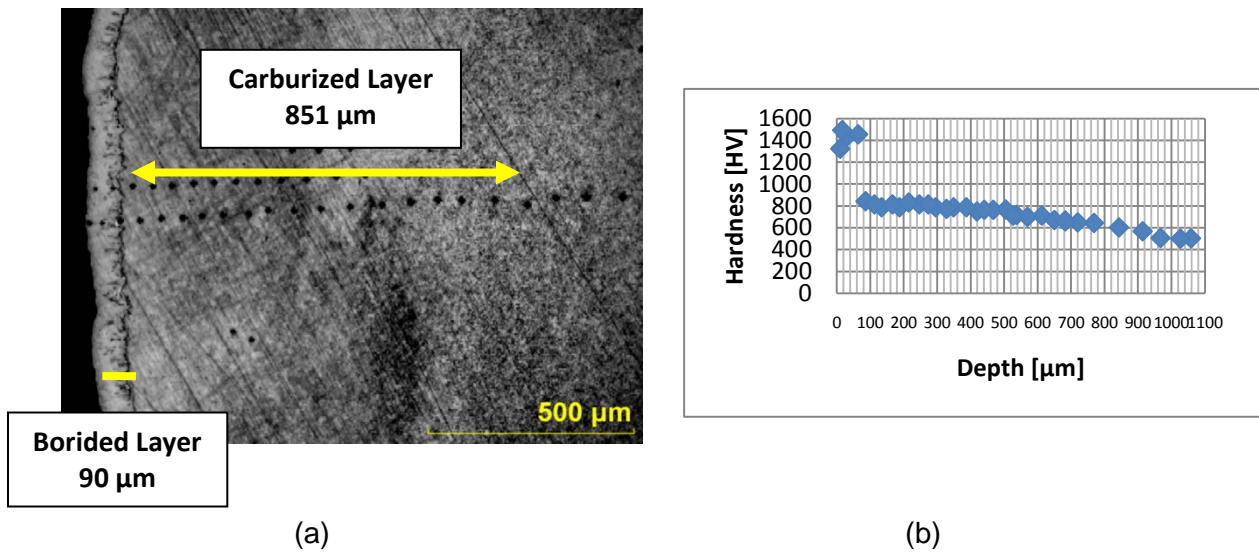


Figure 21. (a) Cross-sectional image of a carburized and then ultra-fast borided knife guard that was subjected to hardening heat treatment after boriding and (b) microhardness profile of the same sample as a function of depth from surface.

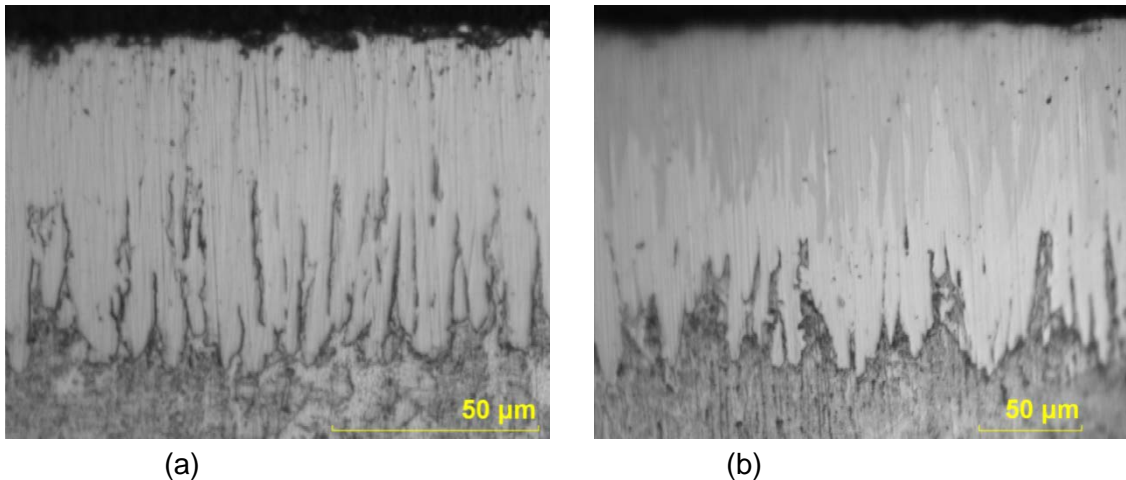


Figure 22. Cross-sectional images of boride layers consisting of (a) single Fe_2B phase and (b) dual $\text{FeB}+\text{Fe}_2\text{B}$ phases used in the stress measurement experiments.

Table 1. Residual compressive stress levels in boride layers.

Boride Layer Composition	Compressive Stress
Single-phase Fe_2B (Fig. 22a)	-2156.1 MPa
Dual-phase $\text{FeB} + \text{Fe}_2\text{B}$ (Fig. 22b)	-1108.9 MPa

Design and Construction of Industrial-scale Boriding Unit

The most important goal of our project was to design and construct an industrial-scale boriding unit that could process large batches of all kinds of industrial parts at once. Accordingly, throughout the project and in particular during Year 2, we spent a considerable amount of time in designing and constructing a large-scale boriding furnace that would allow industrial-scale production. In fact, by the end of the second year, we completed the design phase of such a furnace and then initiated its construction. As a case study, in such a system, Bodycote wanted to be able to treat as many as 100 knife guards per hour so that up to 300,000 parts could be treated per year. Some of the most important design considerations for this unit were: design of interior fixtures and part holders; electrification of the entire system; assembly and integration of control units; furnace shape, size, and capacity; many types of materials to be used in the construction; furnace cap with suitable part holders and busbars, etc. Figure 23 shows a schematic of initial fixture designs for achieving a high production capacity of 96 knife guards per run. The interior dimensions of these designs are 43 in. (length) x 57 in. (width) x 54 in. (depth). They can easily handle up to 96 large cutters or other parts that our industrial partner is currently boriding with their pack-boronizing process. The current protocol calls for 15-min electrochemical boriding and then soaking or holding in the molten electrolyte for up to 1 h and then cooling down or quenching. The total processing cycle is expected to be about 2 h, and if operated in full capacity, the unit would be able to treat more than 300,000 industrial parts per year.

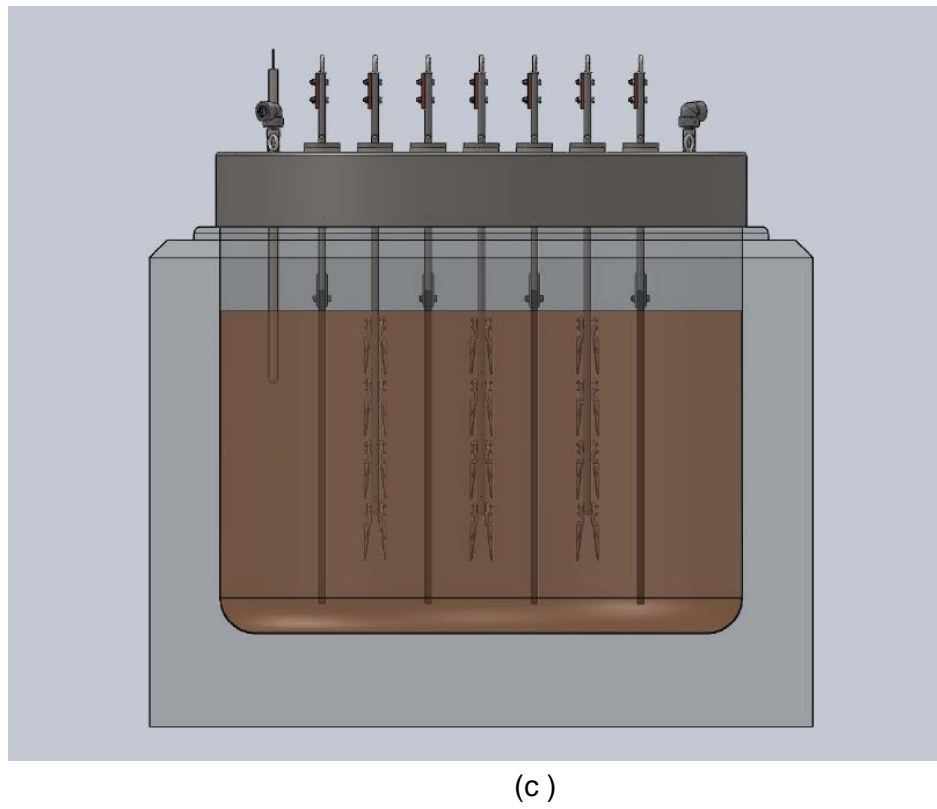
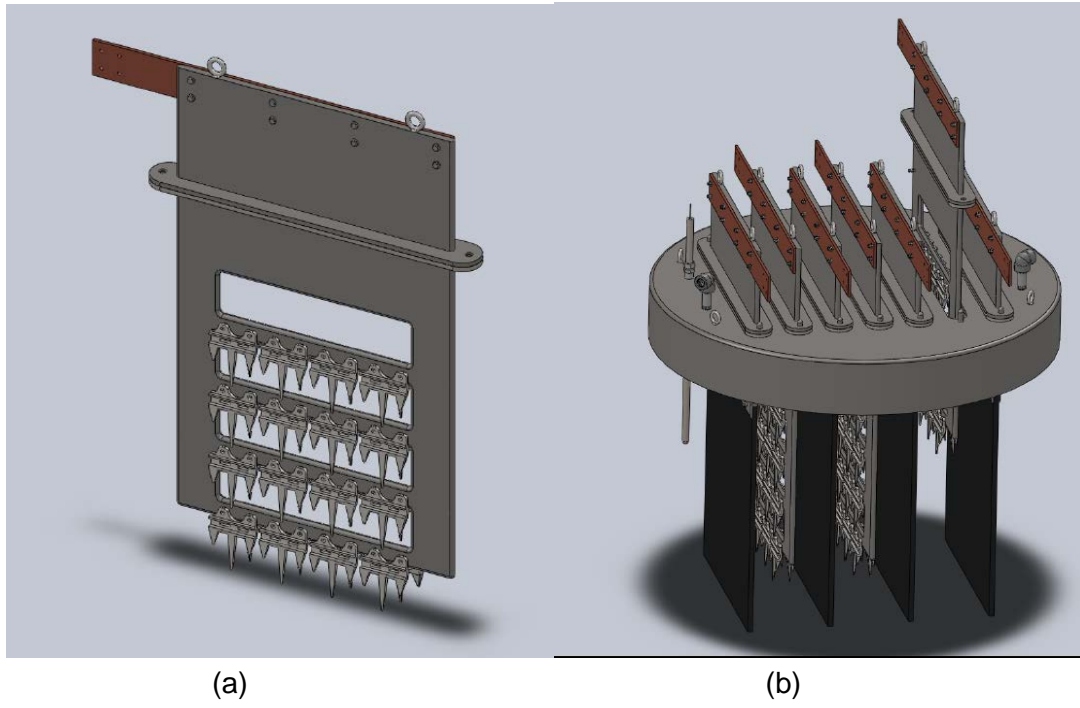


Figure 23. Schematic of (a) fixture for 32 knife guards in one holder, (b) complete design for 96 knife guards, and (c) knife guards loaded in the production-scale unit.

For the shape and size of the production-scale boriding unit, we have also considered multiple furnace designs that could process up to 300,000 industrial parts per year in full-scale operation. To demonstrate the feasibility of designing and eventually building this boriding unit, we first designed a square furnace pot in order to provide additional flexibility and larger capacity (if needed) for the treatment of all kinds of industrial parts. Figure 24 shows a schematic illustration of such a furnace.

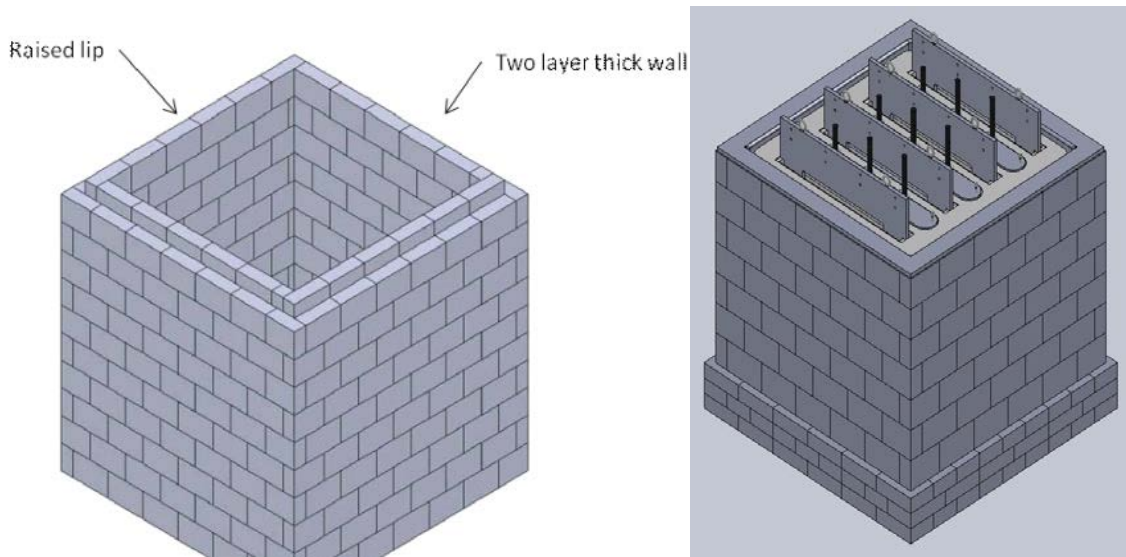


Figure 24. Schematic of square production unit (open top on left and fully assembled with top furnace cap assembly on right).

Initially, we considered a graphite sheet against the side walls of this system as a liner or even as an additional cathode, but after further discussion with the furnace manufacturer, we decided to use high-quality SiC bricks for the construction of the interior walls, and then use a highly insulating secondary outer wall instead. Our design effort was not limited to the furnace shown in Fig. 24 but included other critical/important components and fixtures that are needed for the boriding operation. Figure 25 shows the furnace cap assembly that we designed. A few possible holders with actual parts attached to them are also shown in Fig. 26. For this boriding unit, we selected graphite anodes in the form of rectangular sheets facing the parts to be treated. These anodes will remain in the molten electrolyte while the cathode assembly with various parts will be inserted and removed from the electrolyte by a special crane.

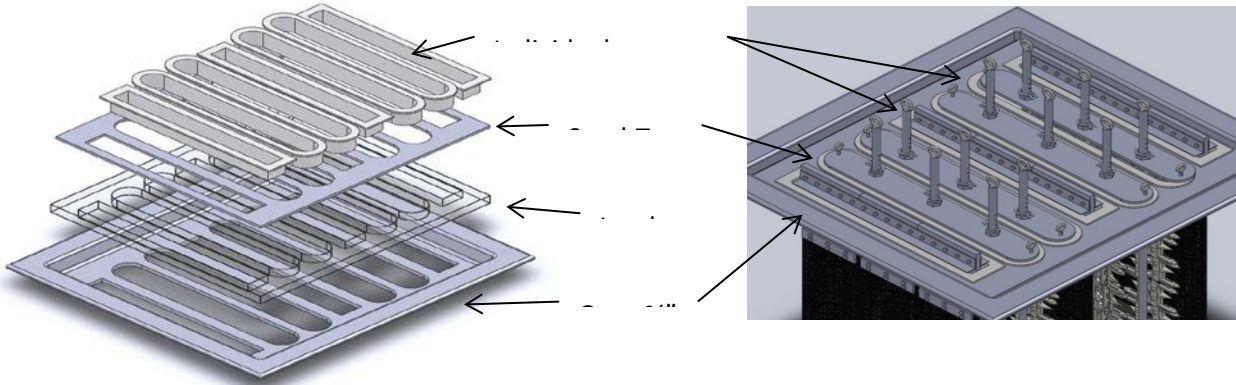


Figure 25. Schematic of furnace cap assembly showing details of electrodes and other fixtures.

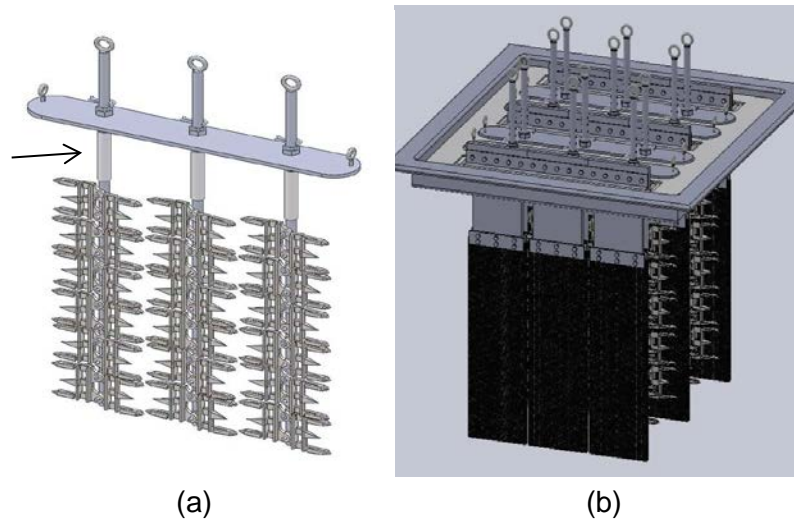


Figure 26. Schematic of (a) individual part holder (cathode) and (b) graphite anode and cathode assemblies together.

Selection of materials for the anode, cathode, and part holders, as well as furnace walls (including top cover), was extremely important for achieving long life and high resistance to heat and corrosive/oxidative attacks from the molten borax. Accordingly, we had to perform numerous material compatibility tests on many candidate materials in which the smaller boriding units were used to determine what materials would be most appropriate (long lasting) for different parts and sections of the full furnace assembly. In addition, we completed long-duration material reliability studies under a wide range of operating conditions to ensure that these materials would not degrade or develop problems during actual operations. In a few cases, we artificially created extreme boriding conditions to see if some of the critical components of the ultra-fast boriding unit would fail or develop problems due to a sudden change in operating conditions. Among the many brick materials for the construction of the boriding furnace, we had to determine which ones would show the least chemical or corrosive reactivity when in contact with molten electrolyte. To that end, we tested a variety of oxide, nitride, and carbide-based ceramic bricks, different classes of steels, and even some superalloys.

Studies toward the selection of the best material for part holders and other components that would come into contact with molten borax yielded only a few possibilities. In general, most candidate materials we tested showed a strong tendency to react with borax and contaminate

the electrolyte. For example, while running boriding experiments with some of the candidate steel materials, we ran into a discoloration/contamination problem. Specifically, in boriding experiments using these fixtures, we noticed a dramatic change in the color of the molten electrolyte, especially when solidified. The color was not opaque or white (typical of borax) but greenish, as shown in Fig. 27. Such a contamination was a major concern, since it had also slowed the boriding process. We had never encountered this problem before. Upon detailed chemical analyses of the discolored or contaminated electrolyte by energy dispersive X-ray spectroscopy (EDS) and inductively coupled plasma (ICP) spectroscopy, we found that this problem was primarily due to the chromium in the welding material. Apparently, it was leaching out of the welded area and reacting with the electrolyte to cause such a discoloration. The detrimental effect of chromium was confirmed further when we ran some experiments with candidate materials made out of stainless steels and chromium-containing superalloys. They too caused greenish discoloration of the molten electrolyte. In addition, we determined that 316 grade stainless steel was the most resistant to heat and corrosive attack, so we decided to use this material for the fixtures and other parts that would come into direct contact with molten borax.

In another study, we tested numerous brick materials for their durability and performance characteristics against the molten borax. These would have been used for the construction of the first wall in the interior section of the boriding furnace. In particular, the corrosion resistance of these bricks in and around the splash zone where molten borax meets air in the furnace was a major concern. In our earlier studies with smaller furnaces, this zone was where the most corrosive attack had occurred. When tested in air, the corrosive attack was severe, but we felt that purging nitrogen through the system and driving air out would probably solve the problem. Accordingly, we ran numerous tests to determine the effect of nitrogen flow on the durability of candidate crucible materials. As long as sufficient flow of nitrogen was maintained over the molten electrolyte, there was no adverse effect on these candidate materials, but when this flow was stopped or drastically reduced, some hot corrosion problems occurred on the inner surfaces of the crucible materials. This corrosion was more pronounced in and around the splash zone near the top surface of molten electrolyte.

To ascertain the adverse impact of oxygen on brick materials, we conducted some in-depth studies and found that oxygen in the surrounding atmosphere was reacting with SiC to result in SiO_x , then SiO_x was reacting with boron and sodium oxides in the electrolyte to form complex silicates, which were, in turn, dissolving in the electrolyte. We also found that the types of brick and binder materials were also important for corrosion performance. For example, if we used a crucible material that was made of porous SiC along with some oxide binders, the durability was poor. These oxide binders may have also played some role in the poor corrosion resistance of the crucible materials. In other experiments using high-quality SiC brick with nitride binders, this problem was solved: there was no evidence of hot corrosion (even when nitrogen gas flow was reduced drastically, and hence high levels of oxygen were perhaps present). Figure 28 shows one of the bricks tested in molten borax with no evidence of hot corrosion. Graphite crucible worked well in our smaller boriding units as long as the nitrogen gas supply was sufficient. However, this material also ran into some problems when nitrogen flow was restricted, and hence oxygen was present in the environment. Specifically, we found that oxygen was gradually reacting with graphite and thus causing wall thinning, especially near the splash zone. We concluded that the use of high-quality SiC materials in combination with some nitrogen flow would be the best solution in terms of the reliability of brick and anode materials in a production-scale boriding unit.

In search of lower cost but higher quality/durability crucible materials, we also performed extensive tests with other candidate materials that were recommended by companies that are active in molten salt furnaces. In our hot corrosion tests, the recommended brick materials failed very quickly by rapidly dissolving in, or adversely reacting with, the molten electrolyte. We cut these bricks into rectangular slabs and immersed them halfway into the electrolyte for several hours. As shown in Fig. 29, there was a significant amount of material loss at or near the splash zone. Again, in a production-scale system, the use of high-purity SiC bricks or crucibles was the most logical choice. Also, these studies further confirmed that maintaining an inert environment on top of the electrolyte is important and will increase the durability and hence reliability of the whole boriding system.



Figure 27. Electrolyte contamination problem, evidenced by greenish color upon solidification.



Figure 28. Surface condition of a high-quality, dense SiC brick after 72-h continuous testing in molten electrolyte. No evidence of brick failure or corrosion in and around the splash zone.

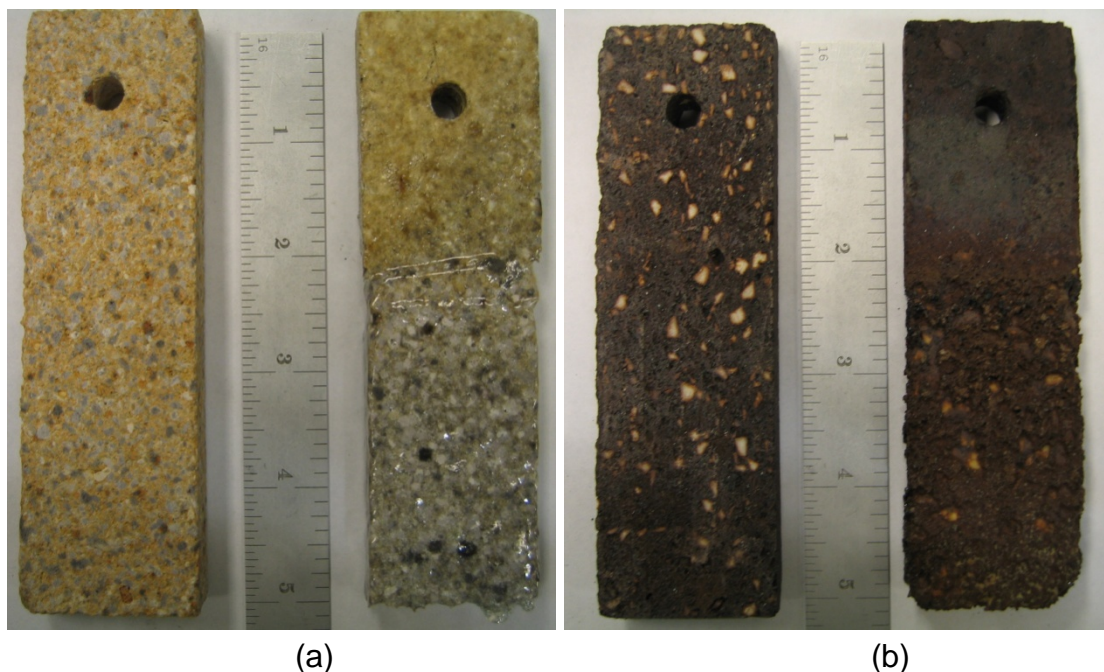


Figure 29. Surface condition of (a) KX-99 (aluminum silicate-based brick) and (b) Narmag 60 (MgO and Cr_2O_3 -based brick) after 3-h testing in molten electrolyte. Both of these bricks failed and corroded away rapidly. In the case of Narmag 60, we also had the same discoloration problem (most likely due to Cr_2O_3).

Besides the interior brick material, we also needed other support material for the wall construction. We could not predict how long the wall structure would last since it was the first of its kind. To avoid leakage, we had to build the wall to be as strong as possible, taking into consideration the many possibilities and worst-case scenarios. Therefore, we had to develop barrier layers beyond the SiC walls on the side and bottom of the furnace, as shown in Fig. 30. These layers required high resistant to hot corrosion and little or no adverse reaction or chemical dissolution if and when there is direct contact with molten electrolyte. Major experimental works required for the construction of furnace walls are discussed below.

(i) *Selection of Sand Layer (Reaction Zone)*

A sand layer was needed in the reaction zone to provide containment of any penetration through the interior SiC walls and to serve as a flexible back-up for SiC bricks should they expand or contract upon heating or cooling. To find the most suitable sand material, we ran extensive experiments with different kinds of sand. The main purpose of this sand layer was to retard or slow down the spread of molten electrolyte to outside layers, act as a reaction zone to increase the viscosity of molten electrolyte, and promote formation of high melting point compounds in the long run. The sand must have a tendency to react with molten electrolyte and, hence, increase the melting point or its viscosity to slow down or stop melt from spreading any further. We considered several kinds of materials for this zone and performed many material selection/compatibility studies. Among others, we anticipated that sand in the form of alumina powder would be an ideal selection due to its high viscosity and potential for formation of a high melting point compound formation on phase diagrams. Unfortunately, there is not much information in the open literature on the reaction kinetics, viscosity, and final compounds

of the sand materials we had initially screened, but based on our experimental work, alumina sand seemed to perform the best. Upon contact with molten electrolyte, it reacted very slowly with molten borax and turned into a viscous, semi-solid substance. During long-duration experiments (24 to 72 h), the penetration of electrolyte through the alumina powder was extremely slow. Moreover, the melting temperatures of possible aluminum/boron/sodium oxides are all above 1000°C, indicating that as long as the temperature of the melt is kept below this value, this material should be able to slow down or retard borax penetration through the wall structure.

We also completed experiments with silica sand, but the silica reacted readily with molten electrolyte and formed a low viscosity melt. Perhaps, the best suitable powder would have been SiC (since it worked well as the brick material), but it is too expensive. We also assumed that in the long run, SiC could oxidize and turn into SiO₂ and, hence, lose its effectiveness.

Altogether, the entire wall construction consisted of seven layers: interior SiC brick, sand alumina, castable material, interior steel containment, insulation blanket, fire brick, and finally steel casing. Figure 30 is a cross-sectional view of one of the corners of this furnace.

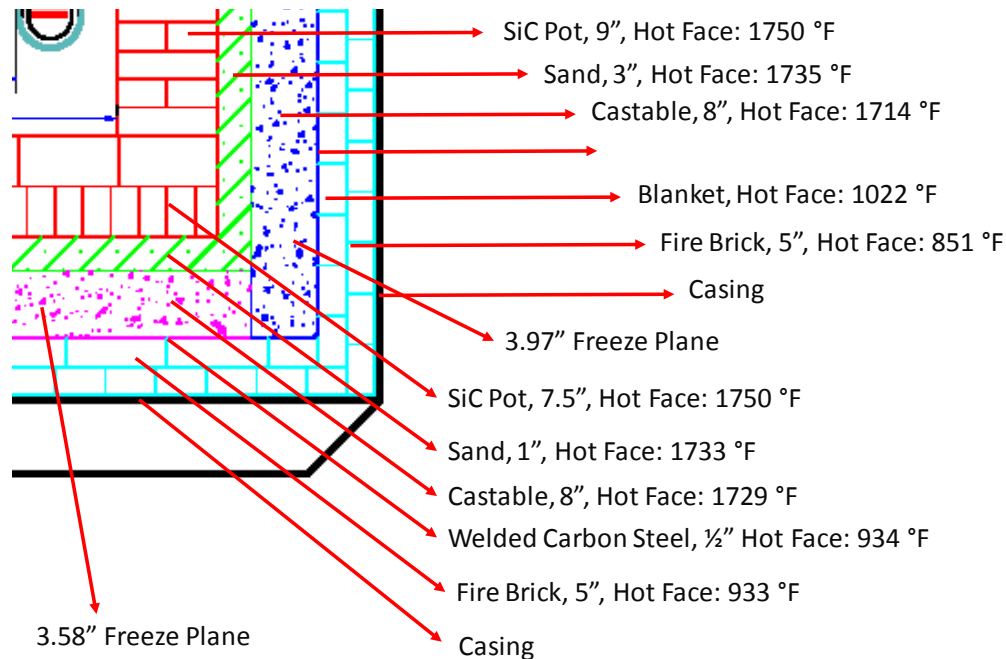


Figure 30. Schematic of furnace wall layers and their functions.

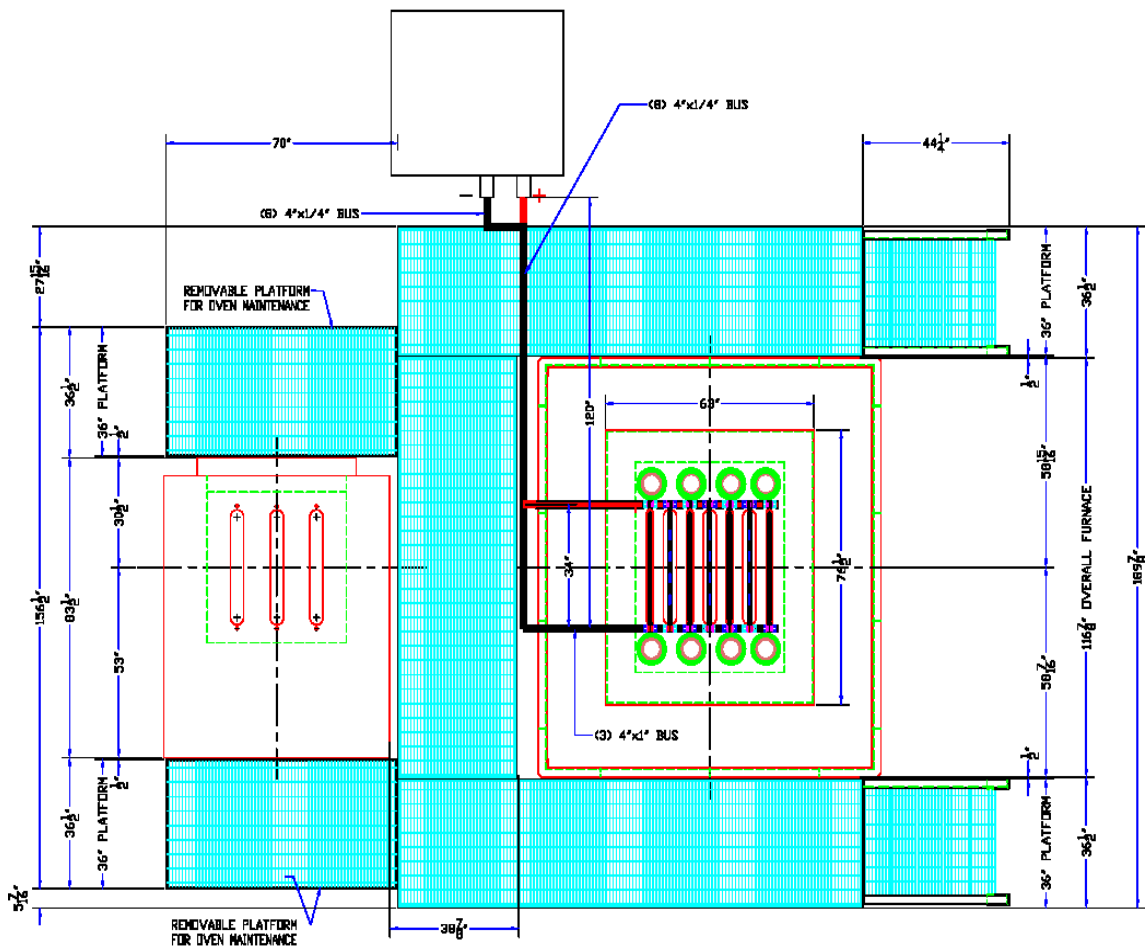
As recommended by the furnace builder, a porous castable material was included after the alumina sand layer. The primary function of this layer was to provide thermal insulation. However, our experiments with smaller bonding units indicated that most castable materials would readily dissolve in the molten electrolyte and hence will not prevent melt penetration through the walls. Based on the results of these experiments, we initially considered moving outside a metal liner to this zone, but during maintenance when the furnace is shut down, this metal liner could have undergone creep or distorted due to exposure to high heat. During cooling, it could have exerted high pressures to the SiC walls and thus caused structural

damage. In the end, we decided to increase the wall thickness of the reaction (sand) zone from 1 in. to 2 in. to provide a better cushion and then place a thinner steel sheet between the castable layer and reaction zone so that any structural damage to the entire wall and further delay of the melt-castable contact might be avoided.

(ii) *Design and Manufacture of Anode, Cathode, Busbars, and Other Fixtures*

Delivering 8000 A current from the power supply to the bridging furnace through the top cover and distributing it to the cathodes (where part holders or fixtures are attached) was a major challenge for us. After many rounds of discussions within our group and with electrical experts from Ajax Electric Co., we developed a final design for the electrification of the bridging unit. Figure 31 shows a schematic of the power delivery systems to the furnace.

When a furnace requires very high currents, the delivery lines are normally kept as short as possible. With this in mind, we placed the power source as close as possible to the furnace. During the unloading of parts, there is always the possibility of molten salt being carried with parts and then dripping on top of the power supply and electrical busbars. Exposing electrical busbars/connectors and the power supply to dripping melt was not acceptable due to safety concerns. For that reason we placed the power supply on the side of the furnace that is away from the loading/unloading path of the parts, as shown in Fig. 31.



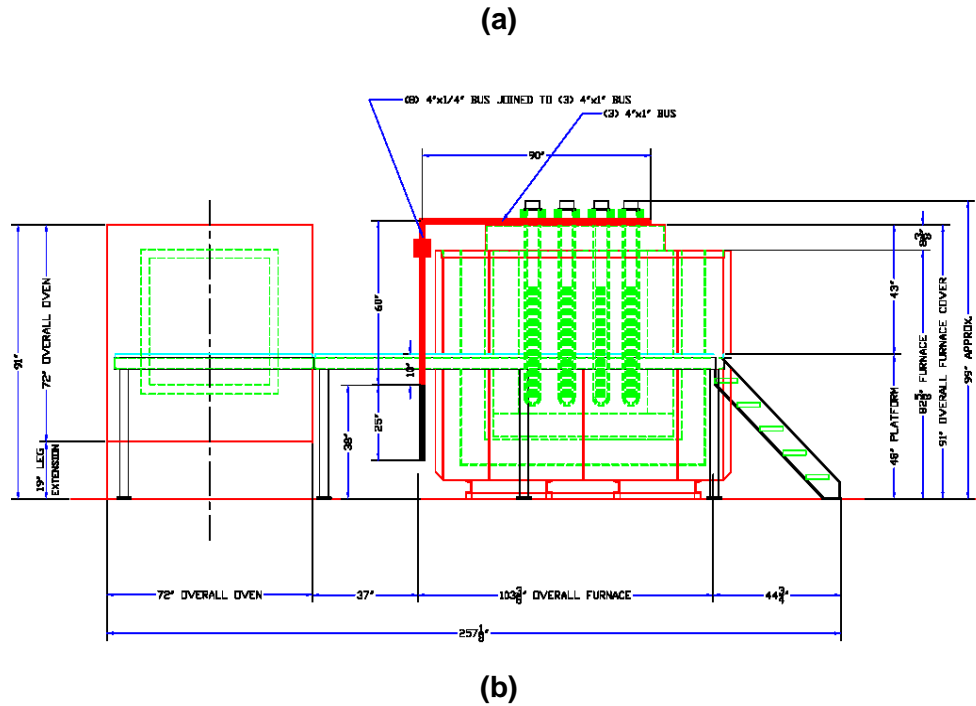


Figure 31. (a) Schematic of electrical connections from power supply to furnace top cover (top view) and (b) side view of the same.

Delivery of electrical current to electrodes will be provided by a series of copper busbars connected to a series of saddles (Fig. 32a). Each side has two saddles (Fig. 32b): one side is electrically connected to a busbar, and the other side is electrically isolated so that the positive and negative poles are distributed to the anodes and cathodes properly.

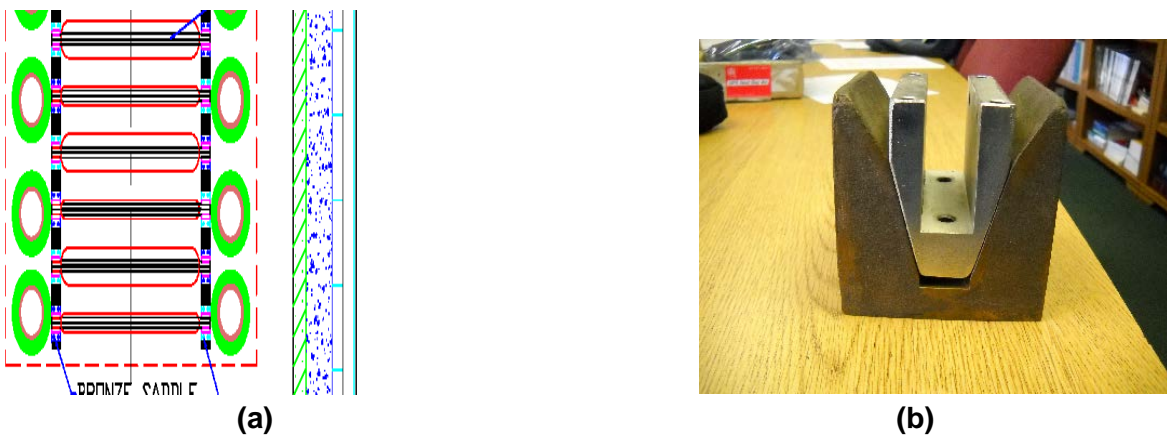


Figure 32. (a) Schematic of power distribution to cathodes and anodes and (b) saddles to be used for delivering power to cathode and anode racks.

The furnace design having been established, we then determined the materials needed for the anode and cathode fixtures. For this purpose, eight materials were selected and tested for their compatibility with the molten electrolyte. The experimental procedure involved anodic and cathodic polarization of rods and/or slabs of each material for extended periods. During these

studies we did not use external protection or masking. After the tests, the rods/slabs were recovered and checked for evidence of wear/corrosion on the material side and contamination on the electrolyte side. The results are summarized in Table 2.

Table 2. Performance characteristics of materials tested for anode and cathode holders.

Material Tested	Anode		Cathode	
	Melt Zone	Vapor Zone	Melt Zone	Vapor Zone
Titanium	--- Eaten away	- Oxidized	--- Drastic decrease in mechanical strength	- Oxidized
Nickel	Significant decrease in mechanical strength	++ No material loss	Some material removal or delamination due to the formation of a thick and brittle nickel boride on outer surface and hence material loss	++ No material loss
Borided Low Carbon Steel	-- Eaten away	++ No material loss	- Decrease in mechanical strength	++ No material loss
Borided High Carbon Steel	N/A	N/A	-- Local spall off	--- Severe oxidation
Borided Stainless Steel (316)	--- Eaten away	++ No material loss	+++ No material and mechanical strength loss	++ FeB to Fe ₂ B transformation observed
BN Spray Coated Stainless Steel (316)	+++ No material loss	+++ No material loss	--- Spalling	+++ No material loss
Aluminite	N/A	N/A	--- Spalling	-- Thick black layer formed
Borided HU Alloy (RA 330 Cast)	N/A	N/A	--- Thick red layer formation and contamination of melt	--- Thick red layer formation and contamination of melt

Note that (-) means unacceptable or bad performance, while (+) means better or acceptable performance.

Based on the results shown in this table, we decided to use borided 316 stainless steel as the cathode material, and spray BN-coated nickel and/or borided 316 stainless steel as the anode material. We will also consider graphite as a backup for the anode material.

As an example, Fig. 33 shows the condition of nickel rods that were tested for their durability under anodic and cathodic polarization. Under both conditions, nickel appeared to work reasonably well.

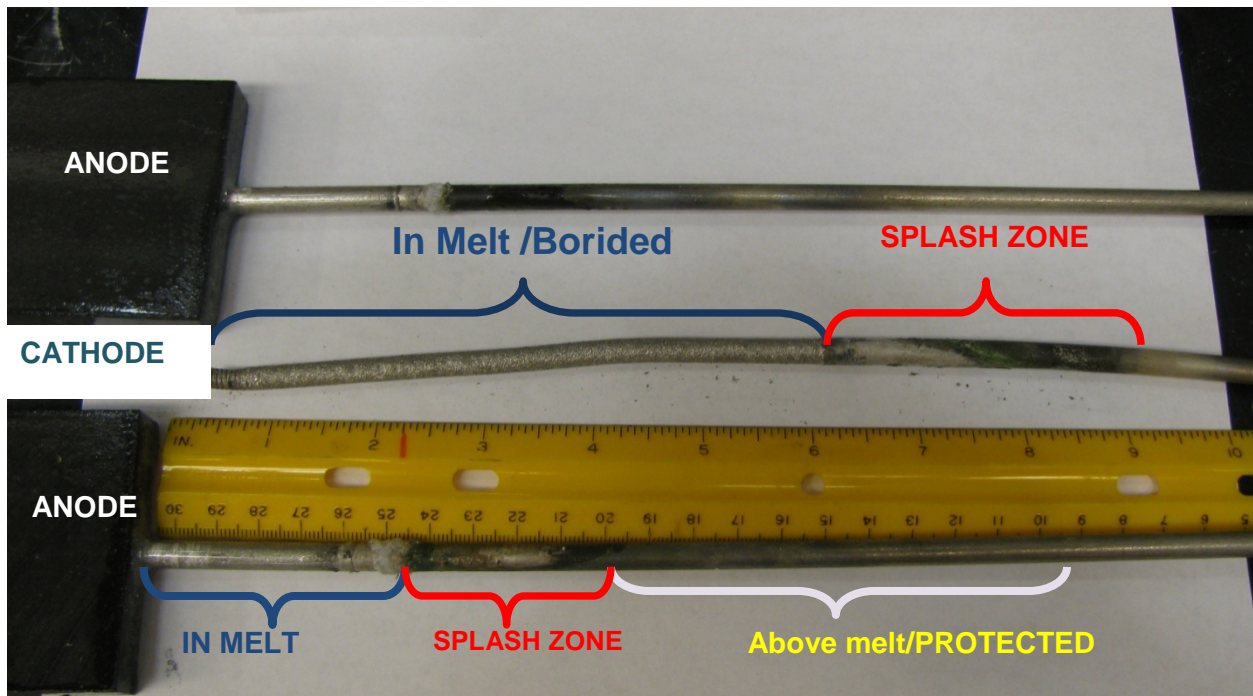


Figure 33. General photos of both nickel rods that were tested as anode and cathode materials.

(iii) *Production-scale Furnace*

Based on the knowledge gained from the studies mentioned above, we selected the various parts and components to be used in the production-scale boriding furnace. Working very closely with the furnace builder, we developed the production-scale furnace that is shown in Fig. 34. The interior section of this unit is 43-in. long, 57-in. wide, and 54-in. deep. The interior walls are made of nitride-bonded SiC bricks that were earlier determined to be the most durable. Beyond the SiC bricks, there are several more layers for thermal management and melt control if the SiC bricks should rupture or leak.

As agreed earlier, this unit was designed to treat 96 large cutters per process run. Our industrial partner had borided these same size cutters by the conventional pack-boriding process, and the turnaround time was more than 10 h. Figure 35 presents an actual photo of these cutters and a schematic of the part holder of our furnace. Each of these holders can handle 8 cutters; there are 12 of these holders, thereby allowing up to 96 cutters per process run. The annual production capacity of this unit for the type of cutters shown was about 300,000. This boriding unit was set up in a strategic location of the high-bay area of Argonne's Building 370. This building is ideal for technology scale-up and demonstration. It has a high capacity crane, which was able to carry the unit into its resting place. This crane will also be used for the

loading/unloading of the workpieces for large-scale boriding. The unit alone is more than 45,000 lb, and when fully loaded with parts and molten electrolyte, the total weight reaches about 60,000 lb.



Figure 34. Completed production-scale boriding furnace. The SiC heaters (three on each side) as well as busbars for electrical connection are on top.

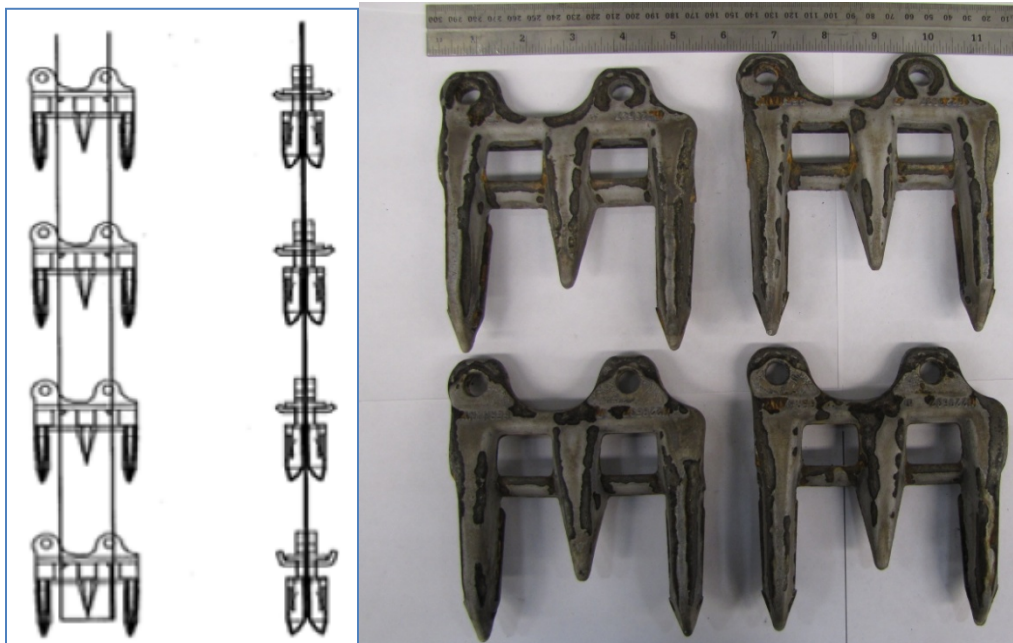


Figure 35. Schematic of part holder and a photo of actual cutters to be used in large-scale boriding trials.

To reduce the time required to bring workpieces to desirable boriding temperature, we purchased a preheating furnace and installed it next to the boriding furnace. Figure 36 shows the top-loading preheat furnace, main power source, and computer-control and data acquisition system that handle both the preheat and boriding furnace, Fig. 37 shows the fully integrated production-scale unit, and Fig. 38 shows borided parts being taken out of the furnace.



Figure 36. Photo of the preheating furnace (top) and the power supply (bottom left) and the computer-controlled power rack (bottom right) as they are being assembled.

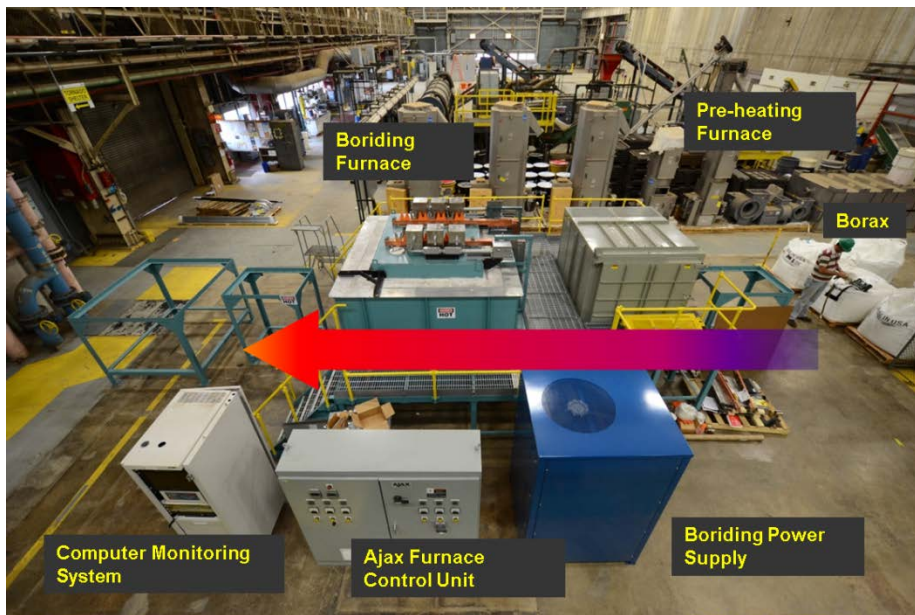


Figure 37. Photo of the fully assembled production-scale boriding furnace.

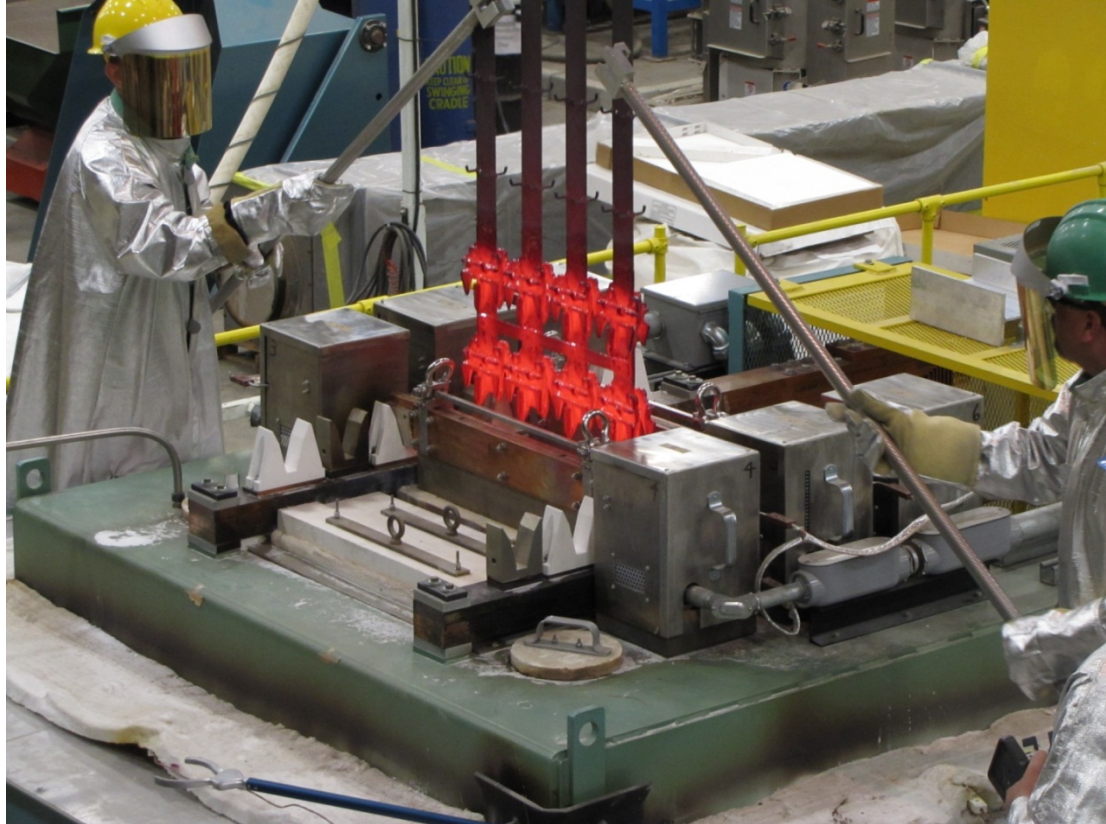


Figure 38. Industrial parts being taken out of the industrial-scale boriding unit after a boriding process.

Boriding of Parts for Field Evaluation

During the project, several industrial parts were borided and delivered to the industrial partner for their internal evaluation and field testing. Figure 39 shows a collection of these parts. A few of them were sectioned and examined by optical microscopy. Figure 40 shows their cross-sectional morphology, confirming a dense and thick boride layer near the surface and on sharp edges.



Figure 39. Borided cutters recovered from pilot-scale boriding furnace (top). Four short (left) and four long (right) middle finger cutters that were borided in 90% borax + 10% sodium carbonate electrolyte at 950°C.

Based upon measurements in the metallographic studies, the thickness of the boride layer was fairly uniform and ranged from about 93 μm to 110 μm . The tip of the cutter finger was well-preserved and looked sharp and defect free. The mechanical hardness of the boride layers was about 1400 Vickers within the borided layer and about 800 Vickers beneath where the pre-carburized layer exists (see Fig. 41).

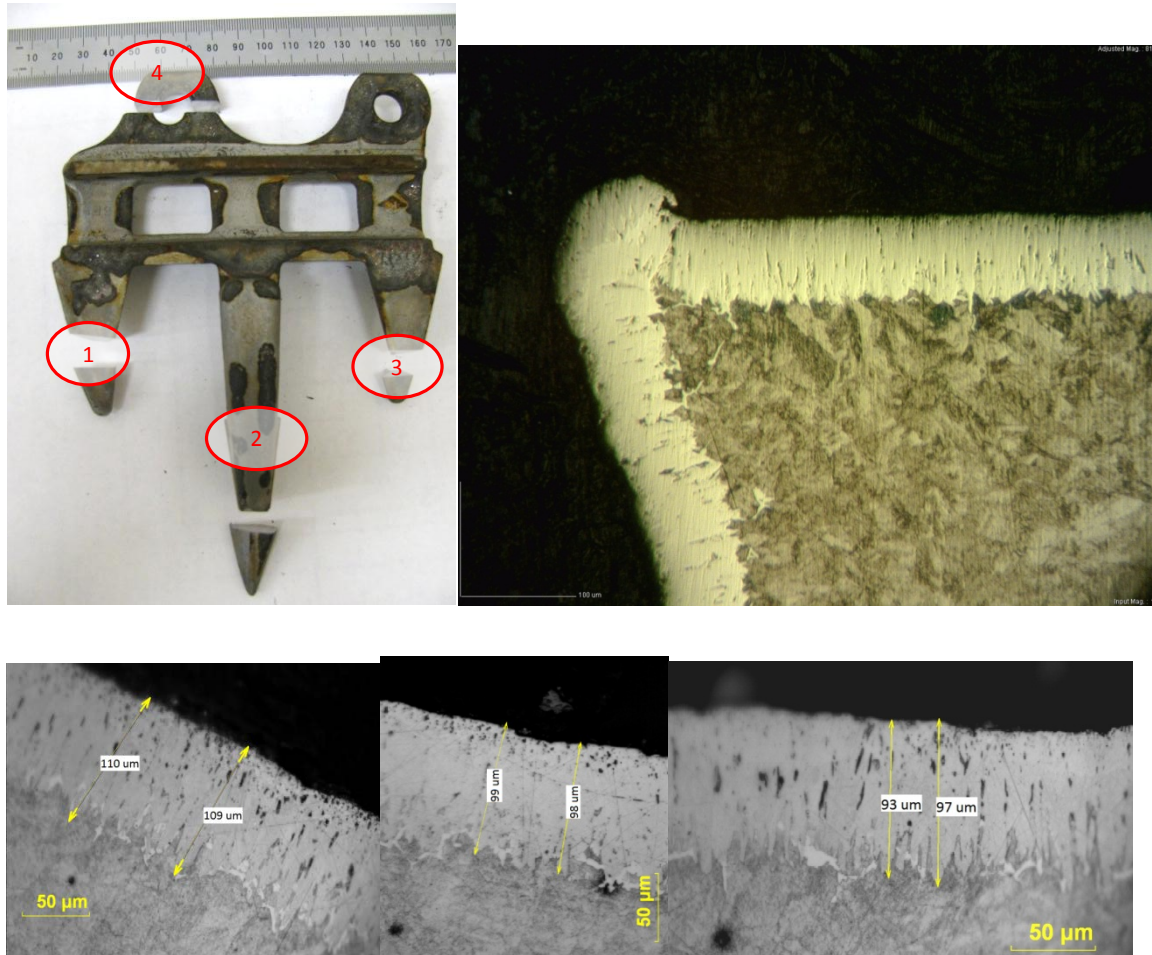


Figure 40. Sectioned cutter and its cross-sectional micrographs from the tip of region 2 (top, right) and from regions 1, 2, and 3 (bottom, from left to right).

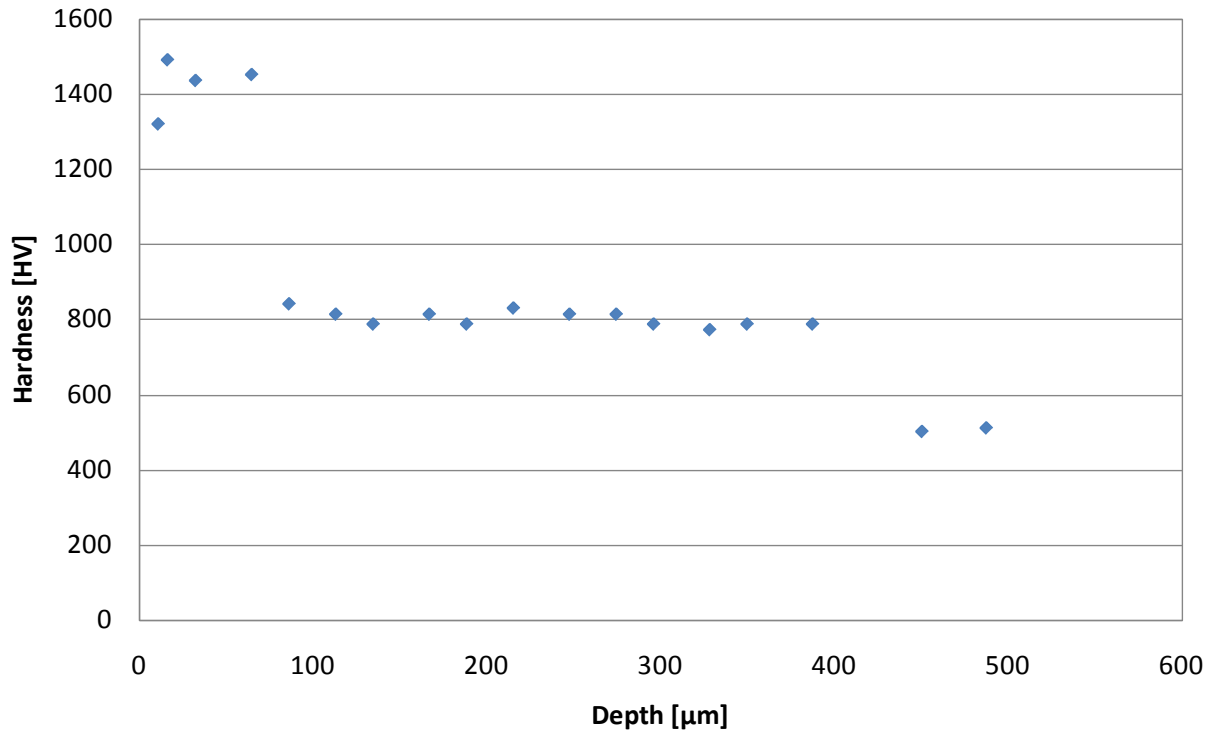


Figure 41. Hardness profile of sectioned John Deere cutter from top surface to interior. Within the borided layer, the hardness is around 1400 Vickers, while that of the carburized layer beneath is 800 Vickers.

Other industrial parts that we borided included some large ball valves used in corrosive and abrasive media (see Fig. 42). Without boriding, these valves were wearing out very quickly, and they had to be changed frequently. They were made of Inconel 600 material and could not be borided with the traditional pack-boriding process. With our process, boriding was simple and fast (less than an hour), and we delivered the borided pieces to Bodycote for field testing. In addition, we treated numerous other industrial parts successfully, some of which are shown in Fig. 43.

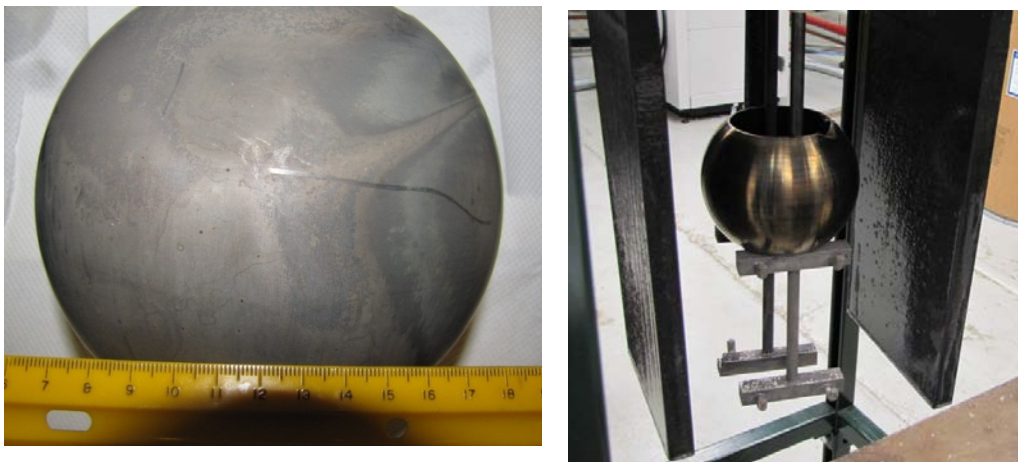


Figure 42. Experimental setup for electrochemical boriding of ball valve (left) and borided ball valve (right) showing clean surface finish after washing in hot water.

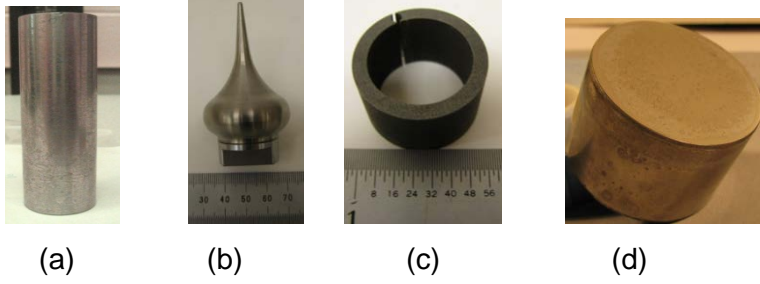


Figure 43. Other industrial parts that were successfully treated by ultra-fast boring: (a) engine piston pin, (b) titanium textile guide, (c) superally bearing component and (d) engine tappet.

Benefits Assessment

The ultra-fast boriding unit scaled-up and demonstrated in this project is a revolutionary surface treatment process with the potential to save a huge amount of energy. It is 80% to 90% more efficient than pack boriding — and it not harmful to the environment (with near zero emissions). At the same time, it reduces costs and increases productivity in a wide range of cross-cutting industrial applications. It will lead to the development of novel surface-engineered metals and alloys with greatly improved corrosion, mechanical, and tribological properties, which can, in turn, increase resistance to degradation in severe industrial operations involving forming, machining, rolling, rotating, and sliding. Production of thick and hard layers in minutes can be considered revolutionary in current surface engineering and treatment fields, where existing boriding processes require many hours.

Our large-scale boriding process has the potential to improve upon all other surface treatment processes, significantly improving the durability and long-term performance of machine components that are subjected to the erosive, corrosive, and abrasive media that are typical of mining, the oil and gas industry, chemical and petroleum plants, forest products, construction, agriculture, and earth-moving operations. It can also enhance the performance and durability of critical tribological components used in transportation and manufacturing sectors. Overall, ultra-fast boriding has the potential to provide significant energy, environmental, and economic benefits to many industrial sectors by increasing energy efficiency, productivity, and environmental compatibility and by lowering operational and maintenance costs (Table 3).

Energy savings and environmental benefits resulting from the uses of large-scale boriding are expected to be huge. Compared to conventional boriding, carburizing, and nitriding, our process is 80% to 90% more energy efficient, and it does not create any in-house greenhouse gas emissions or lead to any type of solid or liquid wastes. By increasing component life, it will reduce the need for frequent part replacement and, hence, curtail the consumption of energy that is needed for the manufacturing of new parts.

Table 3. Key properties of large-scale boriding compared with other surface treatment processes.

Process specification	Argonne ultra-fast large-scale boriding	Pack boriding	Carburizing	Nitriding	Thermal diffusion process	PVD coatings	CVD coatings
Applicable to	Both ferrous and non-ferrous materials	Mostly ferrous alloys, difficult to use for stainless steel and most non-ferrous materials	Mostly low carbon (i.e., 0.1-0.3% C) steels	Mostly low-carbon steel	Mostly steel	All types of ferrous and non-ferrous substrate or material	Mostly, heat resistant steels, cemented carbides, and other alloys
Treatment media	Molten borax	Boron-active powder	Variety (gas, liquid, plasma, etc.)	Variety (gas, liquid, plasma, etc.)	V, Ti, C, etc. containing salt bath	Mild vacuum and plasma	Atmospheric to mild vacuum (plasma in the case of plasma enhanced CVD)

Treatment temperature (°C)	750-1000	800-1150	815-1090	480-590	900-1010	Up to 500	Up to 1000
Energy intensity	Very low (more than 80% more efficient than pack boriding)	Very high	Very high	Very high	Very high	High	High
Carbon intensity or CO ₂ emission	None, or zero	Very high	Very high	Low	High	None	None
Treatment duration (minutes)	15 to 30	480-720	600-1200	360-600	300-600	120-360	600-900
Typical layer thickness (µm)	100-300	50-100	50-1500	2.5-125	20-40	≥10	10-20
Typical hardness (GPa) ^(a)	16-45	10-20	6.5-9.5	6.5-10	10-22	18-40	15-35
Relative wear resistance of treated surfaces	Excellent	Mild to good	Mild	Mild	Excellent	Excellent but limited thickness and lifetime	Excellent
Adhesion to substrates	Excellent	Excellent	Diffusion layer	Diffusion layer	Good	Good	Good
Cost (\$/100 µm/lb)	0.18	1.18	0.34 and 0.67 (for deep case)	0.60 and 0.94 (for deep case)	2.200	Very high	Very high

(a) Typical hardness of fully hardened ball bearing or high-speed tool steels is about 8 GPa or 64 HRC (Rockwell C Hardness).

Commercialization

The ultra-fast boriding technology has been licensed to Bodycote Thermal Processing, Inc. of Dallas, Texas, our industrial collaborator on this project. They are in the process of building multiple production-scale boriding furnaces for large-scale manufacturing.

Accomplishments

Our project has accomplished all of its original goals. The technology has been optimized, scaled up, and transferred to industry for large-scale practice. In addition, it was the recipient of an R&D-100 award in 2012. Our project also resulted in 10 archival journal articles, more than 20 technical presentations, and a patent application along with another invention disclosure. A Ph.D. student (Guldem Kartal) finished her Ph.D. thesis (titled: Boriding of Metals by Cathodic Reduction Method and Optimization of Process Parameters, Istanbul Technical University, December 2011" based partially on the work that she has done on the boriding process; three other summer interns worked on the project during the past summers. Following is a list of publications and presentations that resulted from the work performed under this project.

Publications:

1. "Electrochemical boriding of titanium for improved mechanical properties," G. Kartal, S. Timur, M. Urgan, A. Erdemir, *Surface and Coatings Technology*, 204 (2010) 3935-3939.
2. "Influence of Process Duration on Structure and Chemistry of Borided Low Carbon Steel," G. Kartal, S. Timur, O.L. Eryilmaz, A. Erdemir, *Surface and Coatings Technology*, 205 (2010) 1578-1583.
3. "Kinetics of electrochemical boriding of low carbon steel," G. Kartal, O.L. Eryilmaz, G. Krumdick, A. Erdemir, and S. Timur, *Applied Surface Science*, 257 (2011) 6928-6934.
4. "The Effect of Boron Based Surface Treatment and Nano-particle Lubricant Additives on Friction and Wear Behavior for Wind Energy Applications," A. Greco, K. Mistry, V. Sista, O. Eryilmaz, and A. Erdemir, *Wear*, 271 (2011) 1754-1760.
5. "The growth of single Fe₂B phase on low carbon steel via phase homogenization in electrochemical boriding (PHEB)," G. Kartal, S. Timur, V. Sista, O.L. Eryilmaz, A. Erdemir, *Surface and Coatings Technology*, 206 (2011) 2005-2011.
6. "Ultra-fast boriding of nickel aluminide" O. Kavecioglu, V. Sista, O.L. Eryilmaz, A. Erdemir, *Thin Solid Films*, 520 (2011) 1575-1581.
7. "Electrochemical Boriding and Characterization of AISI D2 Tool Steel," V. Sista, O. Kahvecioglu, O. Eryilmaz, A. Erdemir and S. Timur, *Thin Solid Films*, 520 (2011) 1582-1588.
8. "Evaluation of Electrochemical Boriding of Inconel 600," V. Sista, O. Kahvecioglu, G. Kartal, Q.Z. Zeng, J.H. Kim, O.L. Eryilmaz, A. Erdemir and S. Timur, Submitted to *Surface and Coatings Technology*, 2012.
9. "Electrochemical Boriding of Molybdenum in Molten Borax," O. Kahvecioglu, V. Sista, O.L. Eryilmaz, A. Erdemir, S. Timur, Submitted to *Surface and Coatings Technology*, 2012.

Presentations:

1. "Innovative Surface Technologies for Advanced Engineering Applications: From Super-hard and Low-friction Coatings to Super-fast Surface Treatments," A. Erdemir, George W. Woodruff School of Mechanical Engineering, Georgia Institute of Technology, January 27, 2009.
2. "Advances in Surface Engineering for Advanced Automotive Applications: From Super-hard and -low Friction Coatings to Super-fast Surface Treatments," A. Erdemir, O.L. Eryilmaz, M. Urgan, and K. Kazmanli, S. Timur and G. Kartal, presented at the International Conference on Metallurgical Coatings and Thin Films, San Diego, CA, April 27 – May 1, 2009.
3. "Advances in Surface Engineering for Extreme Tribological Applications," A. Erdemir, World Tribology Congress – IV, September 6-10, 2009, Kyoto, Japan.
4. "Innovative Design Concepts in Surface Engineering for Advanced Tribological Applications," A. Erdemir, Presented at the International Brazilian Conference on Tribology, Rio de Janeiro-Brazil, November 9-11, 2010

5. "Structural and mechanical characterization of electrochemically-borided ICONEL 600," V. Sista, G. Kartal, Q Zeng, A. Erdemir, O. Eryilmaz, G. Krumdick, and S. Timur, Presented at the Materials Science & Technology Conference & Exhibition; Houston, TX ;Oct. 17 - 21, 2010.
6. Effect of Process Duration on Structure, Chemistry, and Mechanical Properties of Borided Low Carbon Steels, G. Kartal, O. L. Eryilmaz, A. Erdemir and G. Krumdick, and S. Timur, presented at the International Conference on Metallurgical Coatings and Thin Films, April 26-30, 2010, San Diego-CA.
7. "Comparison of Abrasive Wear Resistance of Low Carbon Steels Subjected to Carburizing, Nitriding, Nitrocarburizing, and Boriding Treatments," V. Sista, G. Kartal, A. Erdemir, O. Eryilmaz, and G. Krumdick, and S. Timur, presented at the International Conference on Metallurgical Coatings and Thin Films, April 26-30, 2010, San Diego-CA.
8. "Ultra-fast and Thick Boriding as a Novel Surface Treatment for Demanding Tribological Applications," A. Erdemir, presented at the International Conference on Metallurgical Coatings and Thin Films, April 26-30, 2010, San Diego-CA.
9. "Innovative Surface Technologies for Demanding Tribological Applications: From Super-hard and Low-friction Coatings to Super-fast Surface Treatments," A. Erdemir, Mechanical Engineering Department, University of Texas at Arlington, , Arlington, TX, November 12, 2010.
10. "Advances in Surface Engineering for Demanding Tribological Applications," A. Erdemir, 1st International Surface Treatment Symposium, Istanbul Turkey, June 14-18, 2011.
11. "Advances in Surface and Lubrication Engineering and Sciences for Tribological Performance Enhancement," A. Erdemir and L. Ajayi, Presented to Oakland University, Rochester, MI, October 19, 2011.
12. "Advanced Surface Treatments and Nanolubricants", A. Erdemir and A. Greco, NREL Wind Turbine Tribology Seminar, Boulder, CO, November 16-18, 2011.
13. "Innovative Surface Engineering Strategies for Mitigating Wear of Materials Under Extreme Conditions", A. Erdemir, to be presented at the 19th International Conference on Wear of Materials, Portland, Oregon, April 14-18, 2013.
14. "Electrochemical Boriding and Characterization of AISI D2 Tool Steel," V. Sista, O. Kahvecioglu, O. Eryilmaz, A. Erdemir, and S. Timur, presented at 38th ICMCTF 2011, San Diego, CA, USA, May 2-6, 2011.
15. "Ultra-Fast Boriding of Nickel Aluminide," O. Kahvecioglu, V. Sista, O. Eryilmaz, A. Erdemir, and S. Timur, presented at 38th ICMCTF 2011, San Diego, CA, USA, May 2-6, 2011.
16. "The growth of single Fe₂B phase on low carbon steel via phase homogenization in electrochemical boriding," G. Kartal, S. Timur, O. L. Eryilmaz, and A. Erdemir, presented at 38th ICMCTF 2011, San Diego, CA, USA, May 2-6, 2011.
17. "Contact Fatigue Investigation of Borided Steels for Application in Wind Turbine Gearboxes," A. Greco, V. Sista, K. Mistry, C. Barbosa, O. L. Eryilmaz, and A. Erdemir, presented at the 66 Annual Meeting of the Tribologists and Lubrication Engineers, Atlanta, GA, May 15-19, 2011.
18. "The effect of boron based surface treatment and nano-particle lubricant additives on friction and wear behavior for wind energy applications," A. Greco, K. Mistry, V. Sista, and A. Erdemir, presented at the 18th International Conference on Wear of Materials 2011; Philadelphia, PA; Apr. 3 - 7, 2011.

Conclusions

All the tasks and milestones of the project have been realized in a timely manner. The fully developed, optimized, and scaled-up technology has been licensed to the industrial partner. This partner intends to build multiple boriding units for the treatment of all kinds of higher end parts and components in transportation, manufacturing, aerospace, mining, oil and gas exploration, and agricultural areas. With large-scale implementation, huge improvements in productivity, product quality, environmental compliance, and energy efficiency are expected. When we first started this project with only a small unit that could handle 250 g molten electrolyte, we were less than optimistic in terms of making it operational at the 4-ton melt capacity. However, scale-up proved less complicated than we originally thought, especially with the help and practical input of many people at Argonne as well as at Ajax, the company that we contracted for building the furnace (in fact, at the very first trial in most cases). One of the keys to our success was scaling the process one step at a time, i.e., the next furnace being 4 in., then 6 in., then 22 in., and finally the full production-scale unit for large-scale practice. Such a sequential approach to the full-scale furnace increased our confidence and also highlighted some of the major challenges that we might face in a full-scale system. In sum, the project met its objectives, and the technology has been transferred to industry. We are hopeful it will one day help save energy, improve the environment, create new jobs, and help the U.S. economy.

Recommendations

Many high-end or high-value added applications can potentially benefit from our large-scale boring technology. It would be worthwhile to explore some of these possibilities with those companies that are active in the manufacturing sector. Automotive and aerospace parts as well as metal-cutting and -forming tools represent just a few examples where this technology can have a positive impact in the future.

References

1. Sinha, A.K., Boriding (Boronizing) of steels, in *ASM Handbook*, 10th Ed., Metals Park, OH, pp. 437-447 (1991).
2. Matuschka, A., *Boronizing*, Heyden Publications, Philadelphia, PA (1980).
3. Bell, T., et al., eds., *Heat Treating: Including Advances in Surface Engineering*, ASM International, Metals Park, OH (2000).
4. Bhushan, B., and Gupta, B.K., *Handbook of Tribology: Materials, Coatings and Surface Treatments*, McGraw-Hill, New York (1991).
5. Jain, V., and Sundararajan, G., Influence of the pack thickness of the boronizing mixture on the boriding of steel, *Surface Coat. Technol.* 149 (2002) 21–26.
6. Bindal, C., and Erdemir, A., Ultralow friction behavior of borided steel surfaces after flash-annealing, *Appl. Phys. Lett.* 68 (1996) 923.



Energy Systems Division

Argonne National Laboratory
9700 South Cass Avenue, Bldg. 212
Argonne, IL 60439

www.anl.gov



Argonne National Laboratory is a U.S. Department of Energy
laboratory managed by UChicago Argonne, LLC